The
Lawrence Livermore National Laboratory

Research Collaborations Program
For
Historically Black Colleges and Universities

1994–95 Report
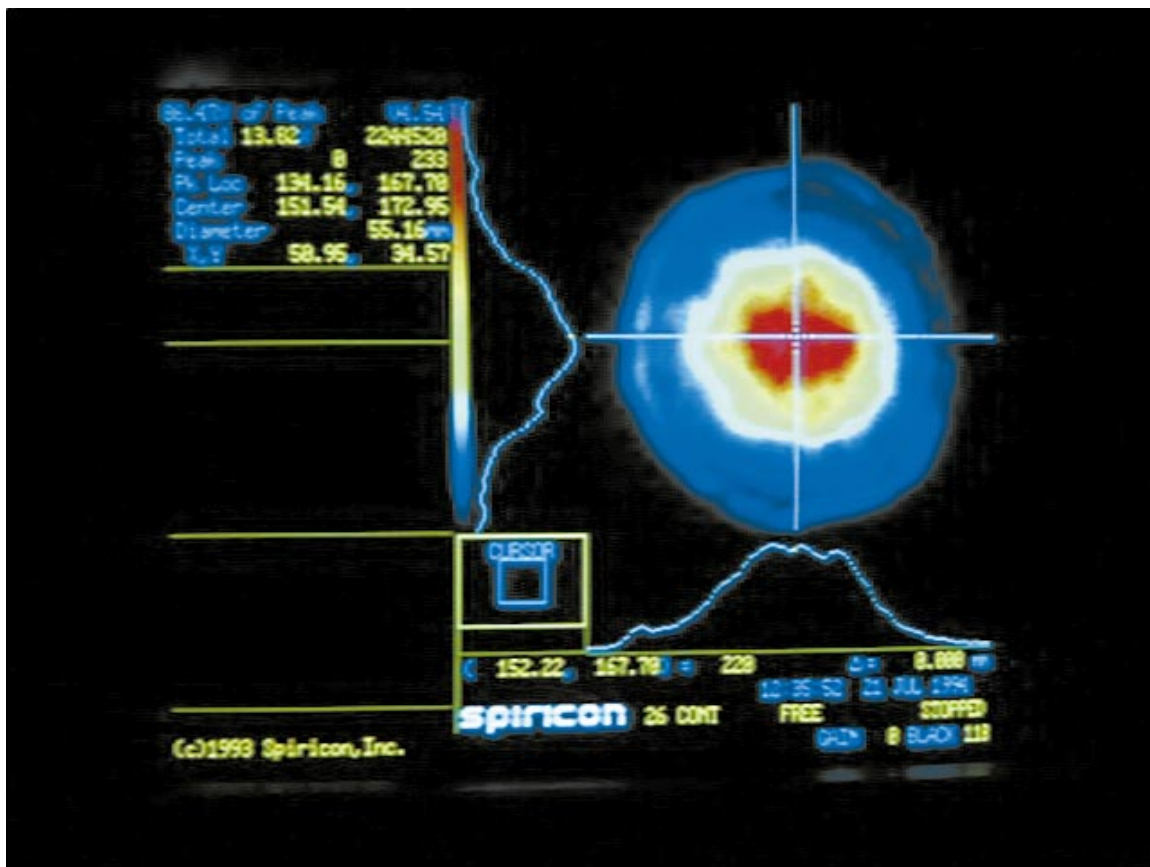

Edited by
Kennedy J. Reed

Lawrence Livermore
National Laboratory

Research Collaborations Program
for Historically Black Colleges and
Universities

1994–95
Report

Edited by
Kennedy J. Reed

Acknowledgments

Section I.   Overview

Introduction

The Lawrence Livermore National Laboratory Research Collaborations Program for Historically Black Colleges was initiated in 1994 as an outgrowth of an effort at Lawrence Livermore National Laboratory (LLNL) to foster productive and mutually beneficial technical interactions between the Laboratory and the nation's Historically Black Colleges and Universities (HBCUs). This effort was pursued through the Affirmative Action and Diversity Program (AADP) and the Education Program at the Laboratory. The goal of the Research Collaborations Program (RCP) is to establish scientific collaborations between accomplished research faculty at HBCUs and Principal Investigators at LLNL, in areas of LLNL Core Competencies.

In conformity with Executive Order 12876, which established the new White House Initiative on HBCUs, the Department of Energy (DOE) has developed a Strategic Plan for Historically Black Colleges and Universities. The vision statement of that Strategic Plan emphasizes the DOE objective of "establishing *effective* partnerships with HBCUs in order to help meet the critical technology needs of our Nation." The RCP is in accord with that statement and provides a mechanism for implementing the vision. The DOE Strategic Plan also lists a set of goals, and Collaborative Research and Development is at the top of this list. The RCP achieves the stated DOE objective of facilitating Collaborative Research and Development efforts between HBCUs and DOE's National Laboratories. The RCP also contributes significantly to accomplishing the stated DOE goals of "Supporting participation of HBCUs in cutting-edge Science and Technology Research and Development" and "Creating Specific Linkages between the Missions of DOE and HBCUs."

Benefits

By linking accomplished HBCU faculty with LLNL researchers actively working in areas of LLNL core competencies, the RCP maximizes the benefits of these collaborations to the Laboratory and to the participating colleges and univerities. Among the major benefits to the HBCUs are:

- Enhanced research capabilities through access to the facilities and expertise unique to LLNL
- Expanded training capabilities, including opportunities for students to work with LLNL facilities and scientists
- Greater visibility in nationally recognized scientific endeavors
- Improved potential for attracting future external funding
- Improved potential for attracting quality students and faculty
- Opportunities for networking and interacting with other HBCUs in the Program as well as with other institutions connected with LLNL

Some of the benefits to LLNL are:

- Basic and applied research to help maintain critical core competencies
- Additional expertise and manpower for basic research through the involvement of professors, post-doctoral researchers, graduate students, and undergraduate students
- Leveraging LLNL facilities for basic research, including computers, equipment, and laboratories
- Impact on future LLNL recruitment needs

During FY94 and FY95, the Research Collaborations Program developed and supported 13 technical collaborations, which have involved 15 professors, 3 post-docs, 4 graduate students, and 22 undergraduate students from 9 HBCUs. These include:

- **Fisk University**, "Development of Cr^{2+}-doped II-VI Hosts as Mid-Infrared Lasers"
- **Morehouse College**, "X-ray Spectroscopy on the Electron Beam Ion Traps"
- **North Carolina A&T University**, "Magnetic Impurity Studies of High T_c Superconductors"
- **Southern University**, "Unified Formulas for Electron-Impact Excitation Cross Sections and Rate Coefficients," and "Development of Solid Electrolyte Materials for Gas Phase Sensors and Fuel Cells"
- **Florida A&M University**, "Turbulence Measurements in Fuel Injection Emulation" and "Charge Exchange Measurements Relevant for Plasma Physics"
- **Spelman College**, "Analytic Basis Set for High-Z Atomic QED Calculations: Heavy Helium-like Ions"

- **Alabama A&M University**, "Investigation of Organic Nonlinear Optical Crystals for Harmonic Frequency Conversion and Electro-Optics"
- **Howard University**, "Studies in High Energy Density Plasmas and X-Ray Fluorescense of Condensed Matter," "First-Principles Computational Studies of Energetic Materials," and "Studies in High Energy Density Plasmas"
- **Prairie View A&M University**, "CP Violation at the SLAC/LBL/LLNL B-Factory"

LLNL scientists participating in these collaborations are from several divisions in four LLNL directorates: Physics & Space Technology, Chemistry and Material Sciences, Defense & Nuclear Technology, and Lasers.

In all of these collaborations, faculty and students from the HBCUs come to LLNL during the summer, and in some cases they also come during their winter and spring semester breaks. The Program encourages the collaborators to continue their research throughout the academic year, on the HBCU campuses as well as at LLNL. To help achieve this, the Program has worked with the DOE Oakland Operations Office to provide grants that cover student salaries and partial release time for professors for the part of the work that is carried out at the universities. The Program has also provided some equipment necessary for performing the research on campus. For example, a computer work station was loaned to Morehouse College so that the professor and students could work at Morehouse on analyses of spectral data from experiments carried out at the LLNL Electron Beam Ion Trap Facility. Computer upgrades have been provided for Prairie View A&M University, giving that research team the capability of working from their university on the simulations, which are part of their contribution to the design of muon detectors for the B-Factory. And computer terminals provided for Southern University and Spelman College enable professors and students at those schools to link with the Super Computers at LLNL and continue performing atomic structure calculations from their campuses in collaboration with LLNL Principal Investigators. In addition, LLNL Principal Investigators have traveled to HBCU campuses to present seminars and to participate in the research at the schools.

Some of the collaborations are multi-institutional. The collaboration with North Carolina A&T University on high temperature superconductors also included work with faculty and facilities at the University of California at Davis. The collaboration with Prairie View A&M University on the B-Factory involves work with the Stanford Linear Accelerator Center and Lawrence Berkeley Laboratory as well as LLNL. And the collaboration with Florida A&M University on "Turbulence Measurements in Fuel Injection Emulation" also involves Sandia National Laboratory. The Program also encourages interaction among the HBCUs where there are similar research interests. This has led to useful interactions between Fisk University and Alabama A&M University in the area of non-linear optical materials.

Student Involvement

Student participation is a critical component of the Research Collaborations Program. For more than a hundred years, Historically Black Colleges and Universities have provided supportive and nurturing environments for the education of African American students in all fields, including the sciences. As a result, a disproportionately large percentage of African American professionals who have earned advanced degrees have received their undergraduate education at HBCUs. The RCP has provided opportunities for undergraduate students, graduate students, and post-doctoral researchers from HBCUs to have significant and enriching research experiences at LLNL and on their home campuses. By enhancing the research capabilities of the HBCUs and supplementing their educational efforts in the sciences, the RCP can have a major positive impact on the training of minority students in these disciplines.

The students who participate in the Research Collaborations Program are chosen by participating professors at their universities. Support from the RCP enables the students to work on research on campus under the direction and mentorship of their professors. The students also come to LLNL with their professors. At LLNL the students have the additional mentorship of the LLNL Principal Invetigators and the benefit of interaction with other scientists involved in the project, as well as the experience of working with the world-class facilities at the Laboratory. The fact that the students are selected by their professors and come to LLNL with someone they know helps to mitigate feelings of uncertainty and discomfort of a strange environment, which sometimes hamper students in summer internships. Since the students are known to

the professors, this arrangement also removes some of the uncertainty inherent in hiring unknown students at LLNL. Furthermore, the students have often had some introduction to the reserach on their campuses before coming to LLNL. With the mentorship of a familiar faculty person, students in RCP are unlikely to fall victim to neglect or avoidance, which in the past has sometimes left summer interns floundering and feeling that their summer work has not been meaningful or productive.

Early in the first summer, it became apparent that many of the undergraduate students who came to LLNL as part of the RCP were under-prepared for participation in the research at the level desired in the Program. For example, some were not sufficiently familiar with angular momentum coupling theory to prepare the inputs for atomic structure codes used in some of the projects. To address this problem, a class in quantum mechanics was organized and taught by LLNL physicists involved in the Program who gave regular lectures and assignments every week. This class was very successful and was continued as a series of lectures in the second summer of the Program. Some of the lectures were given by the HBCU professors as well as by LLNL scientists. Students who returned for a second summer were eager to refresh and expand their knowledge and to help the newer students. They also found these lectures helped in their preparations for the Graduate Record Exams. We were very pleased that, in addition to the students who were part of the RCP, students from other LLNL summer programs learned about these lectures and came to sit in and participate.

Four of the undergraduate students who participated in the Research Collaborations Program have entered graduate programs in physics. One of the students from Spelman College has started graduate school at Ohio State University, and one of the students from Morehouse College is now a graduate student at Wayne State University in Detroit. The student from North Carolina A&T University who worked on the High T_c superconductivity collaboration has received a fellowship and will start graduate studies at Michigan State University; and a student who worked on one of our collaborations with Southern University has started graduate studies in physics at Southern University. All four of these students have acknowledged the positive impact that participation in the RCP had on their decisions to pursue graduate studies in physics and on their preparation for graduate school.

Funding

The collaborations in the RCP have been principally supported through the DOE Defense Programs Office, which provides funds for work with HBCUs through the Education Programs Office at LLNL. However, the participants in the RCP have actively sought support from other sources for the collaborative work and have had some success in this endeavor. In FY94, the collaboration with Florida A&M University was supported by a grant from the DOE Office of Fusion Energy. A grant from the Defense Nuclear Agency was awarded to Howard University as a result of a joint proposal from LLNL and Howard Univerity Principal Investigators, submitted in response to an RFP for the development of High-Z Atomic Physics Models. The Florida A&M collaboration on fuel injection emulators is supported by the DOE Office of Transportation Technology through Sandia National Laboratory.

The participating programs at LLNL have contributed varying degrees of administrative and technical support, as well as use of space and facilities for the collaborations. The Laser Program supported a graduate student from Fisk University during his summer employment at LLNL as part of the collaboration on the development of Cr^{2+}-doped mid-Infrared lasers. Several Principal Investigators at LLNL have also worked with their HBCU collaborators on other joint proposals to be submitted to various agencies, seeking support for continuing and expanding their research. Given the first-rate science that has been produced in these collaborations, it seems likely that some of these proposals will lead to further funding.

The work in these collaborations has already resulted in more than thirty-five papers, which have been either published or submitted for publication in refereed journals or conference proceedings. Research results have also been reported at a number of national and international conferences. All of these joint publications list the HBCU Principal Investigators and the LLNL collaborators as co-authors. The work in the RCP has thus brought recognition to the HBCUs as active participants in significant scientific work, and has also leveraged LLNL facilities and capabilities to carry out basic research that would not otherwise have been accomplished.

Kennedy J. Reed
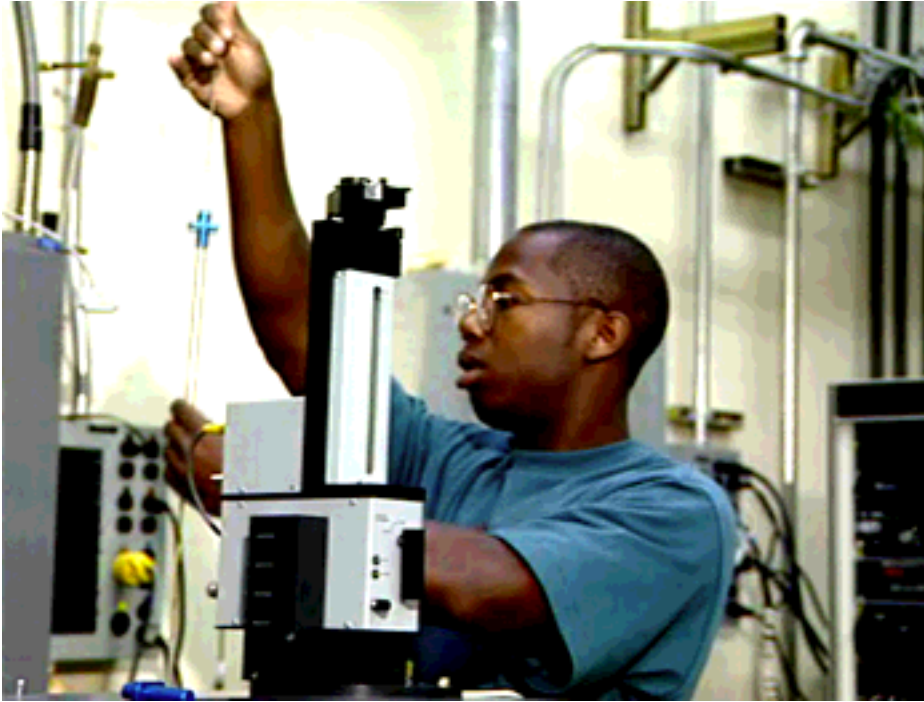
Clarence Buford (student from North Carolina A&T University) in the superconductivity lab at LLNL

Dr. Peter Beiersdorfer (LLNL), seated, and Dr. Augustine Smith (Morehouse College) at the EBIT Facility
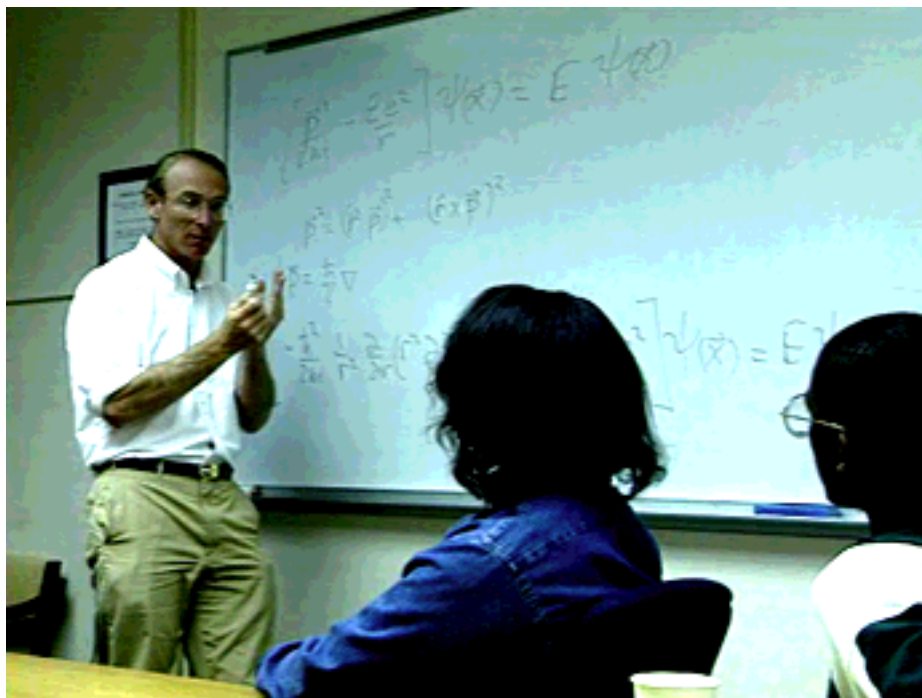
Dr. Neal Snyderman (LLNL) lecturing to students at LLNL.

Aaron Roane (graduate student from Howard University)

Dr. Mau Chen (LLNL) working with students at LLNL
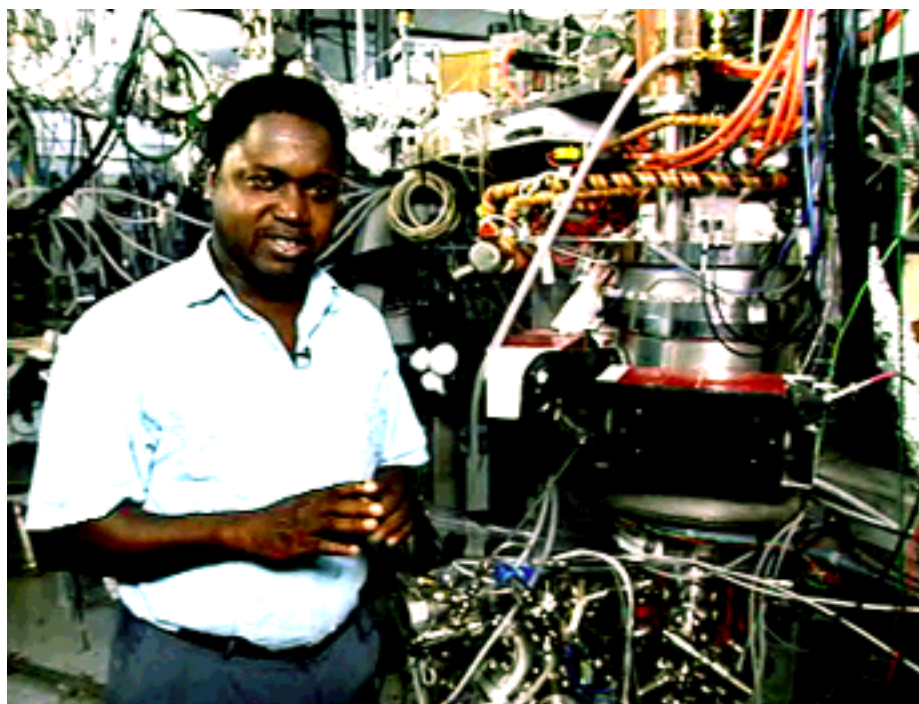
Dr. Augustine Smith (Morehouse College) at EBIT facility
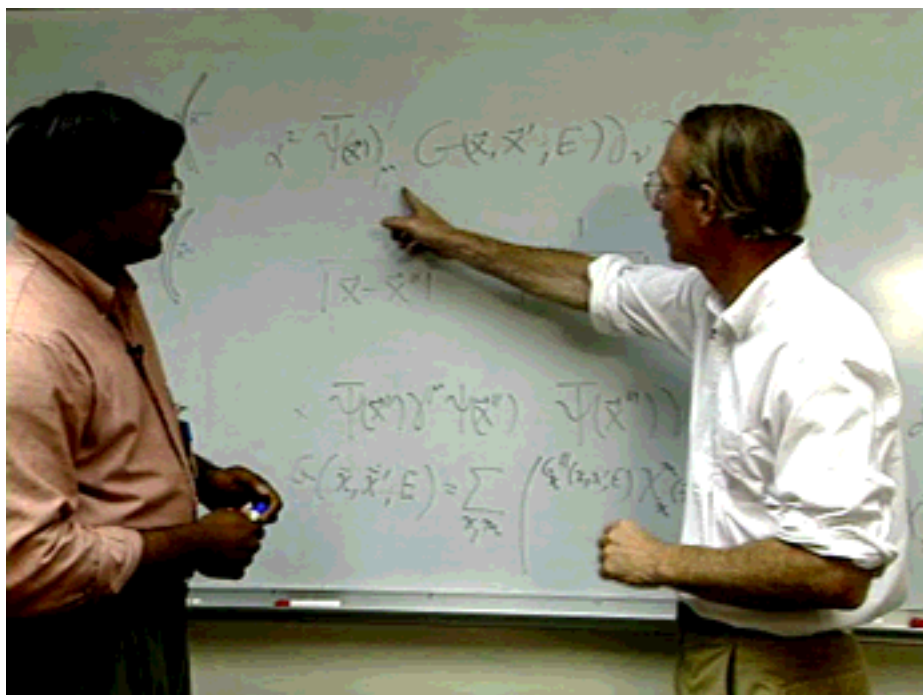
Dr. Derrick Hylton (Spelman College), left, and Dr. Neal Snyderman (LLNL)
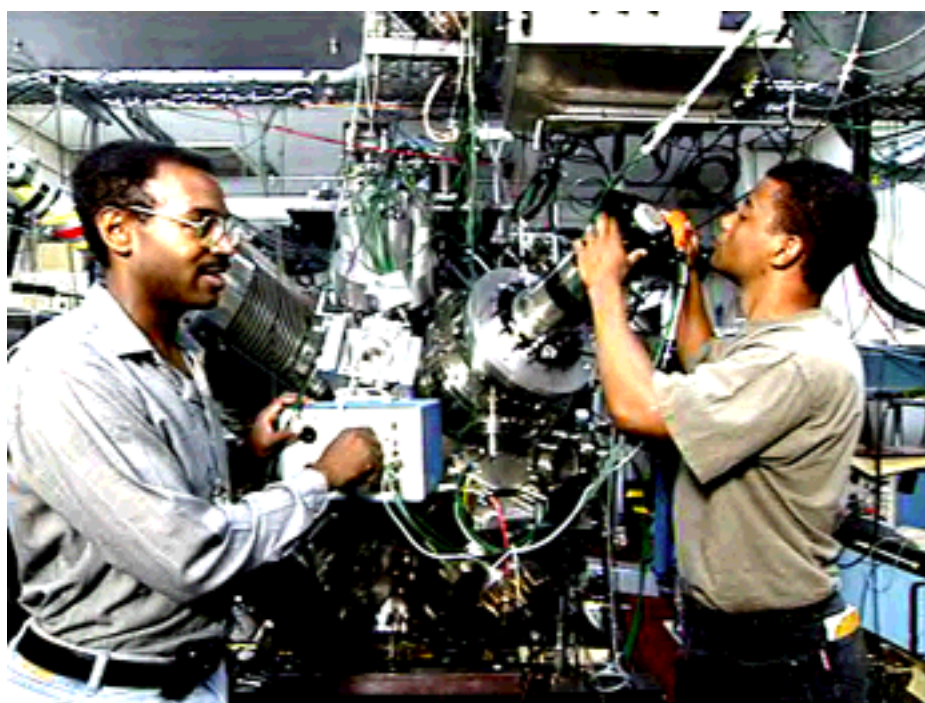
Dr. Ronnie Shepherd (LLNL), left, with Daniel Felten (graduate student from Howard University) at Ultra-Short Pulse Laser Facility at LLNL

Section II.   Research Summaries of Collaborative Projects

Development of Cr^{2+}-doped II-VI Hosts as Mid-Infrared Lasers

Principal Investigators: Arnold Burger (Fisk University) and Stephen A. Payne (LLNL)

Fisk Collaborator: Kuo-Tong Chen

LLNL Collaborators: Ralph H. Page, Kathleen I. Schaffers, and Laura D. DeLoach

Students: Falgun Patel (LLNL), and Southwell Lecointe, Troy Journigan, Yayah Abdul-Aziz, and Jalila Hayes (Fisk University)

Abstract

In FY94 and the beginning of FY95, transition metal-doped II-VI materials were studied at LLNL to determine their potential application as diode-pumped mid-infrared tunable solid-state laser media. The spectroscopic properties of Cr^{2+}-doped crystals of ZnS, ZnSe, and ZnTe were found to be the most favorable; Cr^{2+}:ZnSe and ZnS lased with ~20% slope efficiencies near peak wavelengths of 2.35 mm.

The main goal of FY95 was to do further materials development and laser analysis to increase the dopant concentrations and to reduce the optical losses in the crystals. A joint effort with Fisk University was initiated to study the effects of crystal morphology and doping conditions on the magnitude of losses in the ZnSe and ZnS crystals. We found that the optical losses are highly dependent on Cr-doping techniques and the crystalline quality of the materials. In particular, single crystal ZnSe currently has the lowest losses and the highest efficiency.

Objectives

The initial objective of this project was to develop a diode-pumped solid-state mid-infrared (IR) tunable laser based on II-VI host materials, as recently proposed at Lawrence Livermore National Laboratory (LLNL).

Initially, Cr, Co, and Ni-doped crystals of ZnS, ZnSe, and ZnTe were evaluated spectroscopically for their potential as room-temperature lasers in the 1.5–4 mm region.[1] It was discovered that the Cr-doped materials showed greater potential for tunability, high-gain cross sections, and low nonradiative decay losses, indicating that a favorable system with high quantum yields could be developed. However, at the time the passive losses in the crystals were still too high for practical use.

A collaboration with Fisk University was subsequently established as part of the LLNL Research Collaborations Program (RCP) for HBCUs. The project was aimed at obtaining the optimal concentrations of Cr^{2+} ions and acceptable optical losses in ZnS and ZnSe hosts without compromising the radiative lifetime and quantum yield of the materials. Spectroscopic and laser properties of these two materials were studied further and correlated with preparation methods, such as purification, crystal growth, diffusion mechanisms, and doping conditions. Three types of material are being studied: single-crystal boules grown by seeded physical vapor transport [SPVT] (Eagle-Picher Corporation), poly-crystalline boules grown by the Bridgman method (Eagle-Picher Corporation), and standard window material or pressed microcrystallites (II-IV Incorporated). General applications that will benefit from this research range from areas of spectroscopy (tunable in the molecular fingerprint region), remote sensing, laser infrared radar (in the 2.3 mm atmospheric window), to medical applications such as the development of a "tunable scalpel."

Progress

In late FY94/early FY95, we determined at LLNL that Cr^{2+}-doped II-VI materials showed great promise as diode-pumped mid-IR laser media. They have strong absorption bands in the range of 1.4–2.0 mm, which match the output of strained-layer InGaAs diode lasers.[2] The emission spectra exhibit broad bands centered around 2–3 mm with cross sections of ~75–188 × 10–20 cm^2. Absorption and

emission spectra for Cr:ZnSe are shown in Figure 1. In addition, the similarity of low and room-temperature radiative lifetimes of Cr:ZnS and Cr:ZnSe suggest quantum yields near 100%.

To verify that the spectroscopic properties were consistent with the predicted favorable conditions for lasing, laser experiments using Cr:ZnS and Cr:ZnSe were performed. Both crystals were made to lase at peak wavelengths of ~2.35 μm and slope efficiencies of ~20% using a 7.5% output coupling element. These results were very encouraging, and in conjunction with Fisk University, we began an effort to increase the efficiency of the materials by reducing the optical losses and increasing the dopant concentrations.

Cr-doping of these materials is achieved by direct incorporation into the boules during the growth process and/or diffusion of Cr into prepared undoped crystals at high temperatures. To date, a series of 28 diffusion-doping experiments have been performed at LLNL and Fisk on single-crystal, poly-crystalline, and window material samples of ZnSe and ZnS. The diffusion process requires that extreme care be taken to ensure that contaminants are absent during the experiment. We have also found that Cr-doping concentrations and optical losses are highly dependent on diffusion times and temperatures. Currently, the diffusion doping process, as first demonstrated at Fisk University, has resulted in the highest concentrations of dopant.
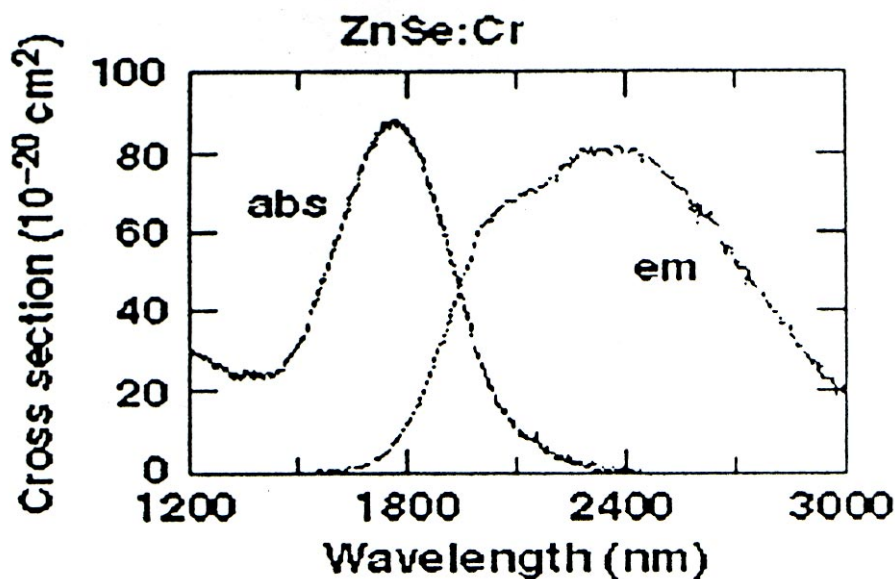
Figure 1. Absorption and emission spectra for Cr²⁺-doped ZnSe.

Spectroscopic and laser performances of the materials studied indicate that optical losses are the lowest in the single-crystal material, as would be typically expected. Laser experiments similar to those described above were performed on a doped single-crystal sample, grown using the SPVT method at Eagle-Picher Corporation. The experiments entailed pumping the material at 1.86 mm with a Co:MgF2 laser with the crystal centered in a nearly confocal cavity. A 30% slope efficiency was achieved from this sample, which is the best to date; a plot of the laser output energy (mJ) versus the pump energy (mJ), with a 6% output coupler, is plotted in Figure 2. [3] In addition, the diffusion-doped polycrystalline and window material shows potential for laser performance and low optical losses, and it is less costly to fabricate when compared to growing single crystals.

The data gathered thus far is encouraging for optimizing the mid-IR laser performance of Cr-doped II-VI materials. This research is ongoing in FY96, and we are confident that further study will provide high-quality material for laser development.
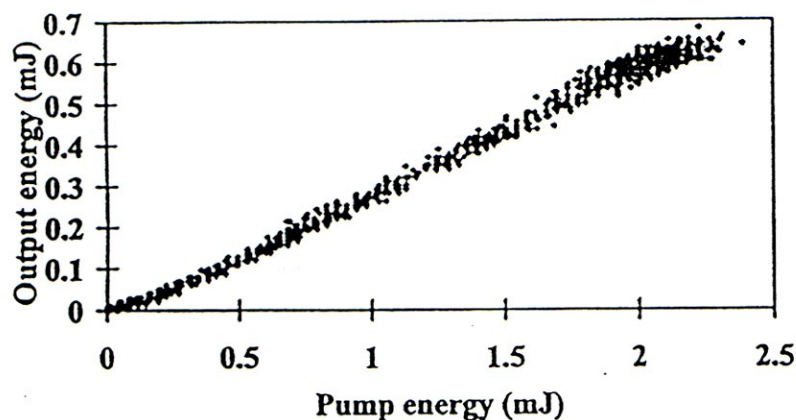
Figure 2. A plot of the laser output energy versus pump energy gives a slope efficiency of 30% for Cr:ZnSe—the highest to date.

References

1. L. D. DeLoach, R. H. Page, G. D. Wilke, S. A. Payne, and W. F. Krupke, "Properties of transition metal-doped zinc chalcogenide crystals of tunable IR laser radiation," OSA Proceedings on Advanced Solid-State Lasers, Vol. **24**, pp. 127–131, 1995.

2. J. S. Major, Jr., D. W. Nam, J. S. Osinski, and D. F. Welch, "High-power 2.0 mm InGaAsP laser diodes," *IEEE Photon. Technol. Lett.* **5**, pp. 594–596, 1993.

3. R. H. Page, L. D. DeLoach, G. D. Wilke, S. A. Payne, R. J. Beach, and W. F. Krupke, "Cr^{2+}-Doped II-VI Crystals: New Widely-Tunable, Room-Temperature Mid-IR Lasers," LEOS '95, San Francisco, CA, Oct. 30–Nov. 2, invited paper, 1995.

X-ray Spectroscopy on the Electron Beam Ion Traps

Principal Investigators: Augustine J. Smith (Morehouse) and Peter Beiersdorfer (LLNL)

LLNL Collaborators: Vincent Decaux, Klaus Widmann, and José Crespo López-Urrutia

Students: Jelani Mahiri (Morehouse), John Autrey (Morehouse), and Michelle Slater (Spelman)

Abstract

In FY 1995, we performed a wide variety of detailed studies of the x-ray spectra from helium-like ions ranging from helium-like Mg^{10+} to helium-like U^{90+}. Our studies include a measurement of the dielectronic satellites pertaining to the $n=2 \rightarrow 1$ x-ray spectrum of helium-like Co^{25+}, which are useful electron temperature indicators in high-temperature plasmas. The measurement focused on accurate determinations of wavelengths and resonance strengths of the dielectronic satellites from lithium-like Co^{24+} and beryllium-like Co^{23+}, and several differences with theory were found. Subsequently, our investigations have shifted to measurements of the satellite spectrum of helium-like Ar^{16+}. These measurements focus on the $n=3 \rightarrow 1$ x-ray satellites that have a spectator electron with principal quantum number $n \geq 3$ and are crucial to the interpretation of spectra from laser-produced plasmas. We also studied the polarization of the x-ray lines emitted from helium-like Mg^{10+}, in order to test the effects of line excitation by a directional electron impact, and we searched for excited-to-excited state transitions in helium-like U^{90+}.

Objectives

The ion and electron temperature and density are crucial parameters that quantify the conditions necessary for achieving thermonuclear fusion, both in magnetically and inertially confined plasmas. Techniques have been developed that rely on the interpretation of the x-ray line emission of highly charged heavy impurity ions to diagnose these plasma parameters. One method, applied extensively in tokamak diagnostics, is to observe the He-α ($n=2 \rightarrow 1$) emission from transition-metal impurities embedded in

the plasma. In the very dense plasmas produced in inertial-confinement (ICF) research, the He-α emission is optically thick, and the He-β ($n=3\rightarrow1$) spectrum of argon or titanium is used for diagnostic purposes. In order to reliably infer the ion and electron temperature and density from such spectral measurements, accurate atomic data are a prerequisite.

The objective of our research is to provide the atomic data needed for the interpretation of the spectral data from fusion plasmas and their use as temperature and density diagnostics as well as for benchmarking atomic physics calculations. Our objective is to perform detailed studies of He-α and He-β spectra of the ions employed in plasma diagnostics by exploiting the precisely controlled experimental conditions provided at the Livermore Electron Beam Ion Trap (EBIT) Facility. Our measurements include line positions, degree of polarization, electron-impact excitation cross sections, and dielectronic recombination rate coefficients. By extending these measurements to selected very high-Z elements, atomic calculations are tested throughout the entire isoelectronic sequence.

Progress

The x-ray emission by dielectronic satellites pertaining to the $n=2\rightarrow1$ He-α spectrum of helium-like ions from the transition metals is an important diagnostic of electron temperature of magnetically confined fusion plasmas that allows the self-consistent modeling of the observed spectroscopic data. Using the Livermore Electron Beam Ion Trap Facility, we selectively excited the dielectronic resonances in helium-like Co^{25+} and lithium-like Co^{24+} and recorded the resulting x-ray emission with a high-resolution crystal spectrometer (Figure 1).

These measurements were started in FY94 and completed in FY95. A detailed analysis provided accurate atomic data on the line position and resonance strengths of the dielectronic satellites. Comparison with different theoretical results indicated several disagreements for several of the satellite intensities, as documented by Smith *et al.*,[1,2] that will significantly improve the accuracy with which the electron temperature can be inferred from the satellite intensity. Our investigations have subsequently shifted to measurements of the dielectronic satellites pertaining to the $n=3\rightarrow1$ He-β spectrum of helium-like Ar^{16+}.[3] The measurements were also carried out at the Livermore Electron Beam Ion Trap Facility. A data set showing the resonance structure in the line emission as a function of electron beam energy is given in Figure 2.
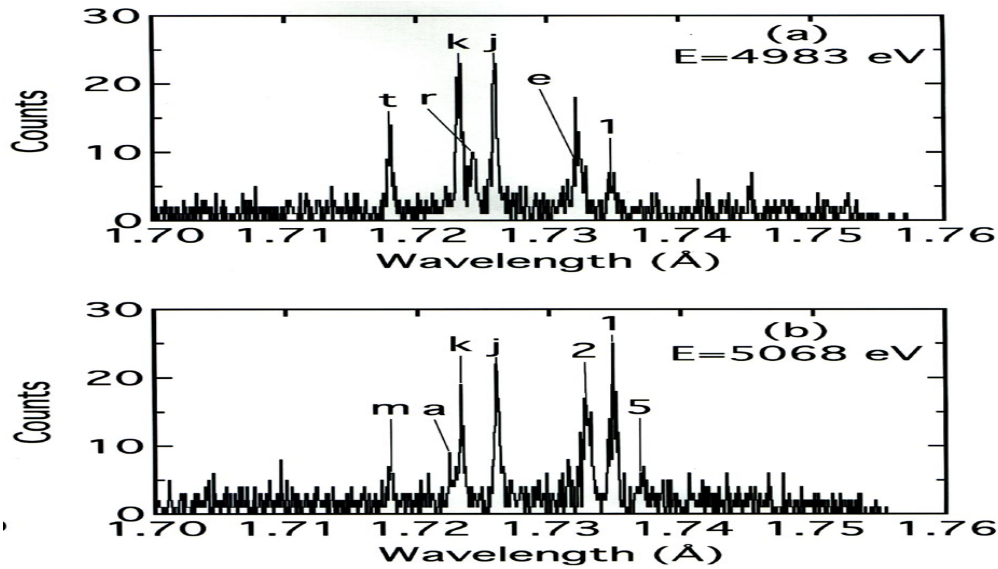
Figure 1. Dielectronic satellite spectrum of helium-like Co^{25+} obtained at electron excitation energies (a) 4983 and (b) 5068 eV. The spectra show that different resonances are excited at different electron energies: (a) has strong contributions from lithium-like satellite lines (labeled with letters), while (b) shows strong beryllium-like satellite lines (labeled with numerals). The resonance energies of lithium-like satellites are overall lower than that of the beryllium-like satellites.
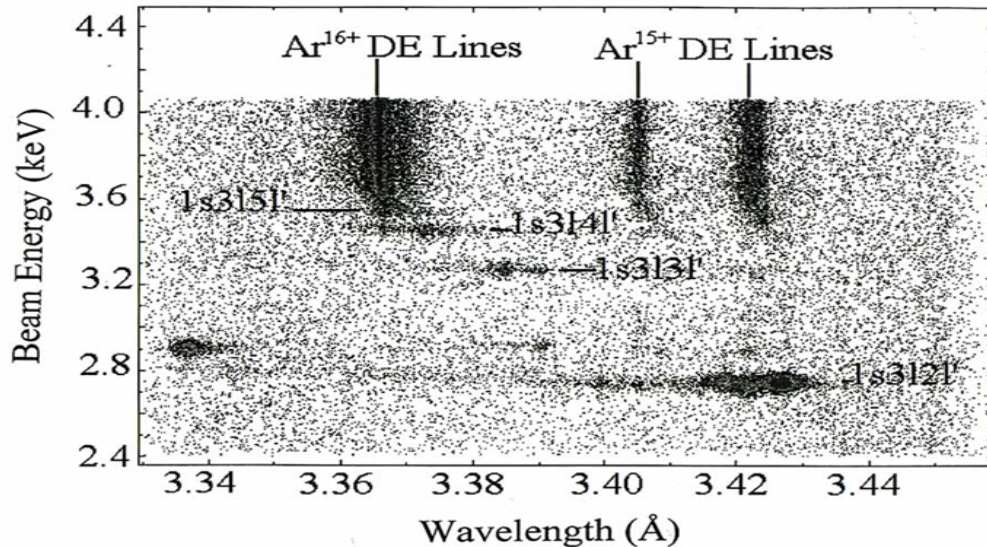
Figure 2. Data set from the EBIT high-resolution Bragg crystal spectrometer showing the x-ray intensity distribution as a function of x-ray wavelength and electron beam energy. The $1s^2$–$1s3p$ $^1P_1$ and $1s^2$–$1s3p$ $^3P_1$ lines in helium-like Ar^{16+} excited by direct excitation (DE) and the associated dielectronic satellite lines of the type 1snl3l' with n=2,3,4,5 and $n{\geq}6$ have been labeled. Also shown are the DE lines in Ar^{15+} and their dielectronic satellites.

Our analysis indicates that the intensity of the $n=2 \rightarrow 1$ x-ray satellites that have a spectator electron with principal quantum number $n \geq 3$ are much larger than commonly assumed from the n^{-3} scaling expected from the n-dependence of the Auger rates.[4] In laser-produced plasmas, these satellites blend with the collisionally excited helium-like lines used to diagnose the electron density resulting in a distortion and shift of the helium-like lines. Since our measurements show that the amount of dielectronic satellites blending with the helium-like lines is larger than generally assumed, a recalibration of the density diagnostic based on the helium-like lines may be necessary.

The intensity of x-ray lines may not be isotropic if the lines are excited in collisions with directional electrons such as those in a beam. Instead, the emitted lines are linearly polarized. We started to study this phenomenon in FY94 by recording the x-ray lines emitted from heliumlike Mg^{10+} under different conditions, and the effects of polari-zation of the lines was immediately obvious. A detailed analysis of the data carried out in FY95, however, showed that the polarization of each line was somewhat less than expected. This is thought to be the result of thermal broadening of the beam that results in a partial depolarization. We are presently working out the theoretical frame-work to determine the amount of thermal broadening necessary to explain the observation. If successful, such measurements will provide a new spectral diagnostic for determining thermal effects on electron beams.

In many cases, our spectroscopic measurements provide wavelength information that is more accurate than data available from any other experiments or from calculations. As a result, our measurements represent benchmarks for testing atomic structure calculations, including the effects of relativity and quantum electrodynamics. In order to provide such benchmarks along the helium-like isoelectronic sequence, we have extended our measurements to include helium-like U^{90+}, i.e., the helium-like ions of the heaviest naturally occurring element. These measurements were carried out at the high-energy EBIT facility using electron beams with 140-keV energy, and very accurate wavelength data were obtained.[5]

References

1. A. J. Smith, P. Beiersdorfer, V. Decaux, K. Widmann, A. Osterheld, and M. Chen, "Measurement of Doubly Excited Levels in Lithiumlike and Berylliumlike Cobalt," *Phys. Rev. A* **51**, pp. 2808–2814, 1995.

2. A. J. Smith, P. Beiersdorfer, V. Decaux, K. Widmann, A. Osterheld, and M. Chen, "Measurement of Dielectronic Recombination Resonances in Heliumlike and Lithiumlike Cobalt," Proceedings of the 19th International Conference on the Physics of Electron Atom Collisions, Whistler, BC, Canada, July 26–Aug. 1, 1995.

3. P. Beiersdorfer, K. Widmann, V. Decaux, A. Osterheld, M. Bitter, K. Hill, S. von Goeler, and A. Smith, "Detailed Measurements and Modeling of the $n=3$ $n=1$ Spectrum of He-like Argon (Ar^{16+})," *Bull. Am. Phys. Soc.* **40**, pp. 179–-1796**0**, 1995.

4. A. J. Smith, P. Beiersdorfer, V. Decaux, K. Widmann, K. J. Reed, and M. Chen, "Measurement of the Contributions of High-n Satellites to the Kβ Lines of He-like Ar^{16+}," *Phys. Rev. A* (submitted).

5. P. Beiersdorfer, S. R. Elliott, A. Osterheld, Th. Stöhlker, J. Autrey, G. Brown, A. J. Smith, and K. Widmann, "Search for 1s2s $^3S1$-$^3P2$ Decay in U $^{90+}$," *Phys. Rev A* (submitted).

Magnetic Impurity Studies of High T$_c$ Superconductors

Principal Investigators: A. B. Kebede (North Carolina A&T University) and H. B. Radousky (LLNL)

LLNL Collaborator: M. B. Bennahmias

UC Davis Collaborators: R. N. Shelton, T. J. Goodwin, and M. McIntyre

Student: C. M. Buford (North Carolina A&T University)

Abstract

During FY94, we conducted a detailed study of the interactions of magnetic impurities in high T$_c$ oxide materials. This is a crucial problem for understanding the fundamental nature of oxide superconductors, as well as having potential technical applications. The nature of the magnetic interactions in the $Pr_{1.5}Ce_{0.5}Sr_2Cu_2Nb_{1-x}TaxO_{10}$ was the main focus of a wide range of magnetic, optical, structural, transport, and thermal measurements performed at Lawrence Livermore National Laboratory (LLNL) and at the UC Davis Department of Physics. The results from the magnetization studies are summaried below.

Objectives

The interplay between Cu magnetism, rare earth magnetism, and high temperature superconductivity in the layered rare earth cuprate systems continues to be a topic of importance for understanding the basic mechanisms of high temperature superconductivity. $Pr_{1.5}Ce_{0.5}Sr_2Cu_2(Nb_{1-x}Ta_x)O_{10}$ is an analog system to the well studied $PrBa_2Cu_3O_7$ system, where all of the samples containing rare earths that form the phase are superconducting, while the Pr material is a magnetic insulator. The $Pr_{1.5}Ce_{0.5}Sr_2Cu_2(Nb_{1-x}Ta_x)O_{10}$ ($0 \le \times \le 1$) compounds display a combination of a weak ferromagnetic component similar to that observed in the Nd_2CuO_4 - type T' structure, as well as a more complicated version of the magnitism observed in $PrBa_2Cu_3O_7$. Our objective was to understand the complex magnetic bahavior in this material, particularly the unexpectedly strong changes observed in substituting Ta for Nb in this material.

Progress

In FY94, we prepared the samples and performed the majority of the magnetization measurements and data analysis. This work was documented in FY95 in *Physical Review B* (in press, February 1, 1996).[1]

Several zero-field cooled and field cooled magnetic spectra for these compounds were obtained for a broad range of applied magnetic field strengths. The results of a compilation of one such data set for the samples used in this study, under the influence of an externally applied field of 500 Oe, are shown in Figure 1. As can be readily seen from this figure, the magnetic behavior of the $Pr_{1.5}Ce_{0.5}Sr_2Cu_2NbO_{10}$ sample (upper left) exhibits two magnetic transitions, while only one ordering peak seems to be apparent in the magnetic spectra for the $Pr_{1.5}Ce_{0.5}Sr_2Cu_2TaO_{10}$ sample (lower right). As one looks at each of the graphs depicted in Figure 1 from the different samples, the magnetic peak at the higher temperature, which has been
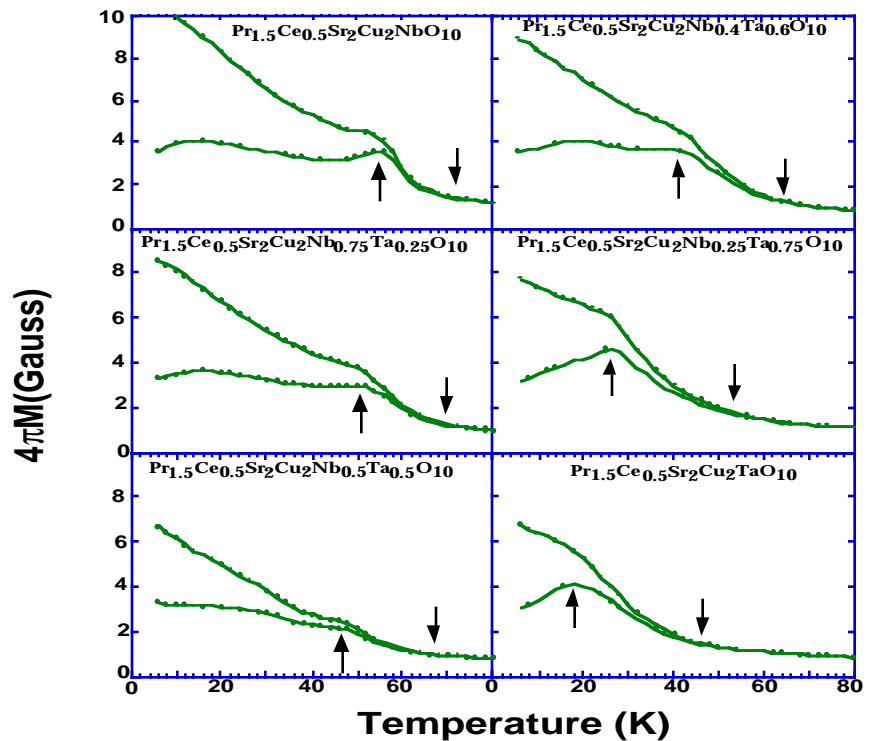
Figure 1. Zero field cooled and field cooled magnetization spectra taken at 500 Oe for the compounds $Pr_{1.5}Ce_{0.5}Sr_2Cu_2Nb_{1-x}Ta_xO_{10}$ (x = 0.0, 0.25, 0.5, 0.6, 0.75, 1.0). The downward pointing arrow indicates the position of the irreversibility temperature and the upward pointing arrow identifies the temperature of the Cu moment reorientation peak.

previously associated to a Cu spin re-orientation and is here identified by the upward pointing arrows, shifts downward from around 56 K in the $Pr_{1.5}Ce_{0.5}Sr_2Cu_2NbO_{10}$ compound to about 19 K in $Pr_{1.5}Ce_{0.5}Sr_2Cu_2TaO_{10}$. The two magnetic peaks are easily discernible in all of these graphs, except for the one corresponding to the $Pr_{1.5}Ce_{0.5}Sr_2Cu_2TaO_{10}$ compound.

In addition , Figure 1 reveals that all of the samples displayed an irreversible behavior characteristic of the weak ferromagnetism in these compounds. The irreversibility temperature, i.e., the tempera- ture at which the zero-field cooled and field cooled magnetization data begin to deviate from one another (identified by the downward pointing arrows in Figure 1), can also be seen to shift towards lower temperatures as one goes across the series of these solid solutions starting from the fully doped Nb end member to the fully doped Ta end member.

The effects on the intensity of the magnetic transition peaks due to varying the applied magnetic field for both the Cu spin transition and Pr ion ordering transition in these compounds is shown in Figure 2
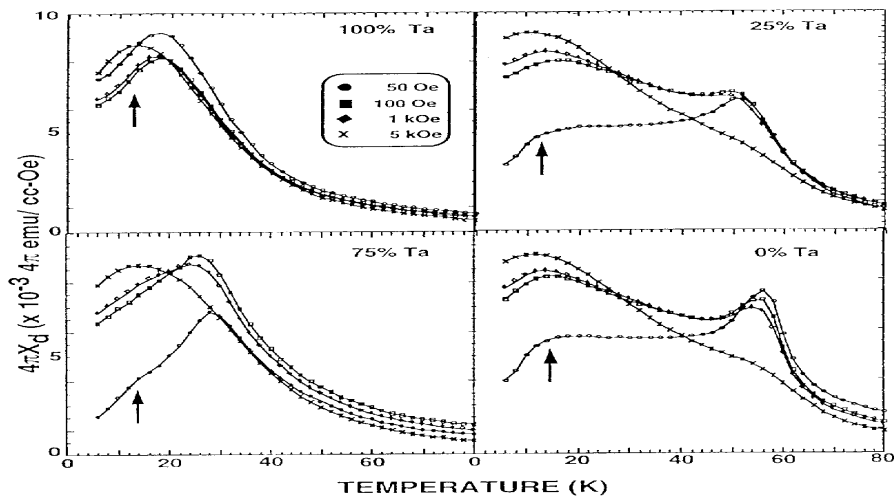
Figure 2. Magnetization spectra showing the changes in the amplitudes of the magnetic transitions associated with the Cu spin transition and Pr ordering for the $Pr_{1.5}Ce_{0.5}Sr_2Cu_2Nb_{1-x}Ta_xO_{10}$ (x=0.0, 0.25, 0.5, 0.75, 1.0). Samples obtained in applied magnetic fields ranging from 50 Oe (circles), 500 Oe (squares), 1 kOe (diamonds), and 5 kOe (crosses). The upward pointing arrow indicates the position of the Pr ion ordering peak. For the fully doped Ta sample, the two peaks fall at the same temperature. At high field, the Cu reordering peak is suppressed, revealing the Pr ordering peak, which remains at 15 K for all of the samples.

over the temperature range 0°K to 80°K. Experimental results obtained from both of the end members and two of the intermediate compounds are shown. The magnetic spectra were obtained in applied magnetic fields ranging from 50 Oe (circles), 500 Oe (squares), 1 kOe (diamonds), and 5 kOe (cross). In all cases, the net effect that is observed upon increasing the strength of the applied magnetic field is a subsequent reduction in the intensity of the Cu spin transition and enhancement of the lower temperature Pr magnetic transition. The peak at 15 K has been assigned to an ordering of the Pr sublattice based on an analogy with the $PrBa_2Cu_3O_7$ and $PrBa_2Cu_2NbO_8$ materials, which have antiferromagnetic (AF) transitions at 17 K and 12 K, respectively.

The behavior of the magnetic peaks as a function of applied field can be simply understood as arising from the convolution of a weak ferromagnetic ordering process riding on a strong paramagnetic background due to the presence of the Pr ions. Upon saturation of the weak ferromagnetic component, and under the influence of strong enough applied magnetic fields, the paramagnetic contribution will then dominate. For example, the observed behavior of the magnetic transition peak from the magnetic spectra obtained on the $Pr_{1.5}Ce_{0.5}Sr_2Cu_2TaO_{10}$ sample, namely an apparent 7 K downward shift in the peak position under the application of a 5000 Oe magnetic field, can be readily explained as a result of a superposition of the Cu spin transition, which is decreasing in intensity with field, and the magnetic ordering peak due to the Pr ions, which increases in intensity. As the two peaks are in close proximity to one another, the apparent shift in peak position would be greater than in the case where the two magnetic transitions were well separated in temperature, as in the case for the fully Nb doped compound. Figure 2 also shows that the ordering peak attributable to the ordering of the Pr ions in these compounds does not change as one goes across the series. This suggests that the presence of Ta or Nb in these compounds does not significantly effect the long-range ordering process of the Pr ions in these crystallographic structures. This peak is identified in the figure with an upward pointing arrow. The temperature at which the inter-layer Cu moment reorientation occurs in these materials under the application of a 500 Oe field, as a function of Nb content, is plotted in Figure 3.

A potential picture we developed for the magnetic behavior in these compounds can be described as follows: (1) from the results of our previous neutron diffraction measurements, the Cu moments order antiferromagnetically below 250 K, while the Pr ions follow a Curie-Weiss behavior; (2) below some characteristic temperature, 130 K in the case of the fully doped Nb material, a subtle structural distortion occurs, inducing a weak ferromagnetic component via an oxygen mediated exchange interaction between the AF-aligned Cu moments, inducing the formation of domains within these compounds (in each domain the Pr ions experience an internal field that polarizes the Pr spins); (3) when the internal field becomes strong enough, a restructuring of the domains within these materials occurs, which is detected in the dc magnetization and neutron diffraction data as a reorientation of the Cu spins; and (4) below a characteristic temperature (15 K), the long-range exchange interactions between the Pr ions begin to dominate the effects of the internal fields and the Pr ion's order.
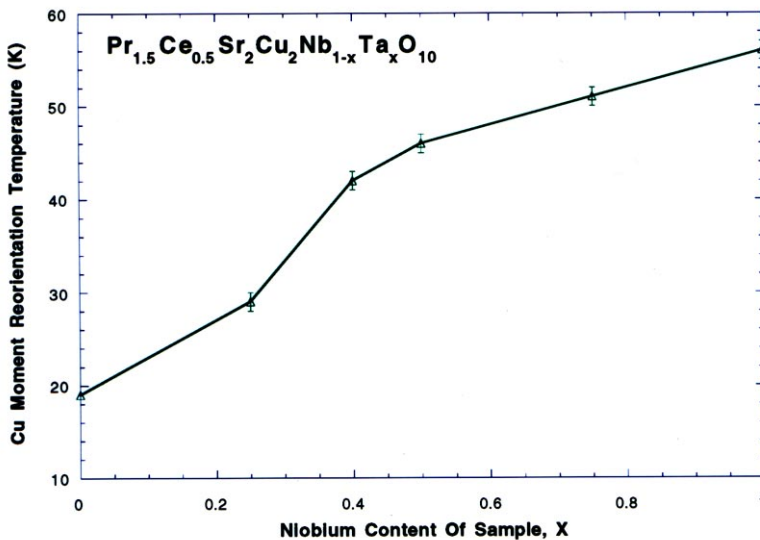
Figure 3. The Cu spin transition temperature as a function of Nb content in a field of 500 Oe. The movement of the peak from 60 K to 20 K in going from Nb to Ta is derived from the data shown in Figure 2.

References

1. M. Bennahmias, H. B. Radousky, M. Buford, A. Kebede, M. McIntyre, T. J. Goodwin and R. N. Shelton, "Magnetic Studies of Ta Doping in Pr$_{1.5}$Ce$_{0.5}$Sr$_2$Cu$_2$(Nb$_{1-x}$Ta$_x$))O$_{10}$," *Phys. Rev. B.* (in press, February 1, 1996).

2. M. J. McIntyre, M. J. Bennahmias, T. J. Goodwin, C. C. Hoellwarth, A. F. Bello, C. M. Buford, A. Kebede, R. N. Shelton, and H. B. Radousky, "Magnetism in Pr$_{1.5}$Ce$_{0.5}$Sr$_2$Cu$_2$(Nb$_{1-x}$Ta$_x$)O$_{10}$," *Bull. of the APS* **40**, 1995.

Unified Formulas for Electron-Impact Excitation Cross Sections and Rate Coefficients

Principal Investigators: Dong S. Guo (Southern University) and Mau H. Chen and Kennedy J. Reed (LLNL)
Students: L. Barlow, V. Walker, and M. Lee (Southern University)

Abstract

Excitation cross sections and rate coefficients including resonance contributions will be computed using the relativistic distorted wave approximation and the multiconfiguration Dirac-Fock method. The analytic formulas for rate coefficients will be determined by least-square fit of the calculated data and should find a wide range of applications in the modeling of hot plasmas produced in either laboratory or astrophysical sources. We implemented a nonlinear least-square analysis code and successfully converted relativistic atomic structure, Auger, and radiative codes to run on work-states in an open computer facility. We also calculated Auger and radiative transition rates for highly-charged ions, which are basic data for computing resonance contributions to electron-impact excitation.

Objectives

Electron-impact excitation cross sections or rate coefficients for highly-charged ions are very important atomic data in the modeling of astrophysical and laboratory produced plasmas.[1] The calculation of excitation rate coefficients including resonance contributions is very difficult and time consuming. In a typical plasma modeling application, rate coefficients for numerous transitions and for many ion stages are usually required. The demands for vast amounts of excitation rate data will make *ab initio* calculations prohibitive. To solve this problem, we shall develop a set of concise formulas for electron-impact excitation rate coefficients including resonances for He, Li, Be, and B isoelectronic sequences. We employ the relativistic distorted-wave method[2] to calculate the direct excitation cross sections. Resonance contributions are calculated separately using a two-step process. The detailed Auger and radiative transition rates needed for calculating the branching ratios will be computed using

the multiconfiguration Dirac-Fock (MCDF) model.[3,4] These theoretical cross sections and rate coefficients will then be utilized in the least-square fitting analysis to obtain the unified formulas.

Progress

We have made good progress in achieving our goal. The students have learned the art of relativistic atomic structure calculations and the skills to carry out relativistic calculations of Auger and radiative transition rates. We have calculated the K-shell Auger and radiative transition rates for 18 ions with $10 \leq Z \leq 95$ in carbon and oxygen isoelectronic sequences using the MCDF model. A post-processing code was written to tabulate the Auger and radiative data. Two manuscripts describing the data are in preparation for publication in Atomic Data and Nuclear Data Tables. Some selected Auger rates are displayed in Figure 1. We have also successfully implemented a version of nonlinear least-square fitting code. A logarithmic χ^2 fitting method was developed to analyze the rate coefficients, which differ by several orders of magnitude between low-Z and high-Z ions.
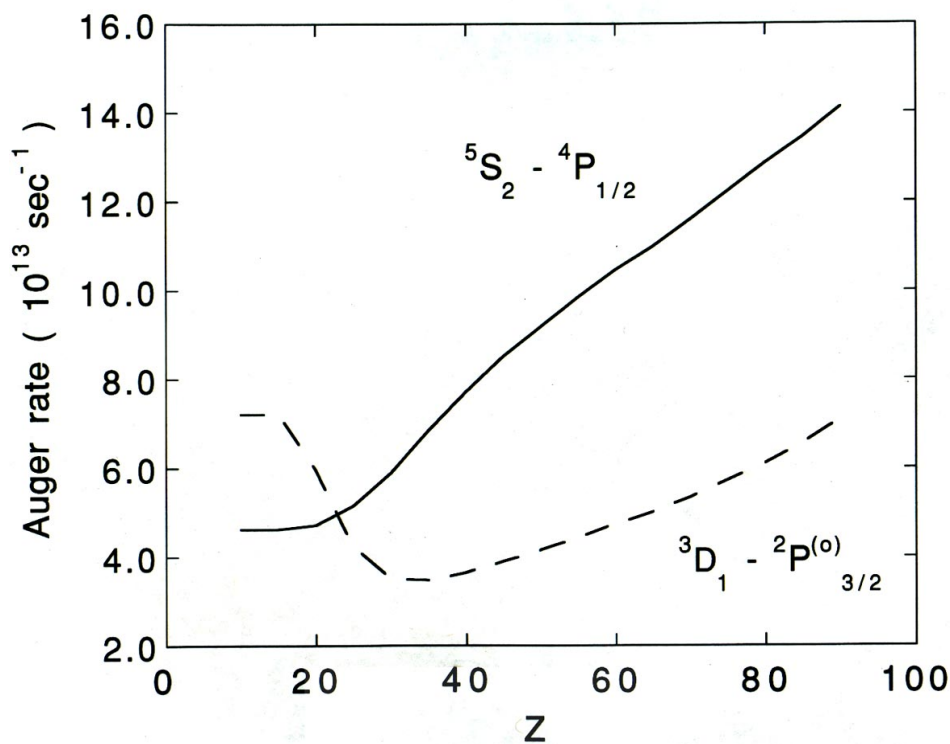
Figure 1. K-shell Auger rate for carbon-like ions as functions of atomic number.

References

1. M. S. Pindzola, D. C. Griffin, and C. Bottcher, "Resonance Contributions to the Electron-Impact Excitation of Ions in the Distorted-Wave Approximation," *Phys. Rev. A*, **32**, p. 822, 1985.

2. H. Zhang, D. Sampson, and R. Clark, "Relativistic Cross-Sections of Excitation of Highly Charged Ions to Specific Magnetic Sublevels by an Electron Beam," *Phys. Rev. A* **41**, p. 198 (1990).

3. M. H. Chen, "Relativistic Auger and X-ray Emission Rates of the ls 2ln 2l-m Configurations of Be-like Ions," *Phys. Rev. A* **31**, p. 1449, 1985.

4. I. P. Grant, B. J. McKenzie, P. H. Norrington, D. F. Mayers, and N. C. Pyper, "An Atomic Multiconfigurational Dirac-Fock Package," *Comput. Phys. Commun.* **21**, p. 2070, 1980.

Turbulence Measurements in Fuel Injection Emulation

Principal Investigators: Joseph A. Johnson, III (Florida A&M University), Charles Westbrook (LLNL), and Robert W. Carling (SNL)
SNL Collaborator: Peter O. Witze

Abstract

The fundamental relationship between standard turbulent parameters, nonequilibrium processes, and the quality of fuel injection in port fuel injected automobiles is not known. New insights on the correlation between this relationship and engine performance could have a profound influence on engine design and on the evolution of appropriate engine performance with respect to both efficiency and emissions. This work involves a systematic investigation on these points using a simulator for a fuel injector and a comprehensive set of turbulence diagnostic and analytical procedures.

Objectives

The first phase of the research will focus on the design of the fuel injection emulation chamber, a fabrication of the mock-up (small scale) fuel injection emulation chamber, the development and calibration of diagnostic procedures appropriate to the proposed measurements, and the implementation of appropriate computer software and hardware.

The second phase, which will overlap the first phase, will show results on turbulence parameter mapping in space and time for the injected gas-vapor mixture and for a temperature sensitivity in the autocatalytic $2NO_2 \rightarrow N_2O_4$ nonequilibrium process at the gas-vapor interface. These measurements will be performed under conditions, at fixed injector expansion rates and fixed injector velocity, which provide the option of a choice of both a turbulent and a nonturbulent region in the expanded jet. Comparisons will be made, when possible, between existing theoretical models and the results of these measurements.

The third phase, which will overlap the second phase, will include the design and fabrication of the full-size fuel injection emulator,

using parameters based on experience obtained on the mock-up emulator. Detailed measurements will be made on all the turbulent parameters, and the influence of Reynolds number variation from changing expansion rates and injector velocities will be determined. All available models will be tested against these results. Moreover, our results will be used to provide new models and specific recommendations for improved engine performance and also to provide the basis for specific proposals for the continuation of the research along the lines suggested in response to the interactions with other interested parties, both in industry and in DOE and/or its designees.

Progress

Using the rapid expansion phase of a pressure-driven shock tube, new unique implications from molecular-based approaches to turbulence have been experimentally confirmed with Mie scattering and real-time trajectory measurements of droplet accretion. Specifically, turbulence has been found to play an important part in the rate of droplet growth. Using the recently available evidence of natural turbulence closure to construct a nonempirical physical model with no arbitrary constants for flow with chaotic behaviors, all classes of droplet growth rate behaviors in the turbulent nonequilibrium environment can be predicted. With this, the development of the MHz optical and particle scattering diagnostics for use in the turbulent burn phase of the combustion cycle has begun. This is to be emulated by a properly configured motored engine aimed, in general, at turbulent manipulation of combustion efficiency.

Analytic Basis Set for High-Z Atomic QED Calculations: Heavy Helium-Like Ions

Principal Investigators: Derrick J. Hylton (Spelman College) and Neal J. Snyderman (LLNL)
Students: Joy Harris and Michelle Slater

Abstract

We have implemented a quantum electrodynamics (QED) perturbation theory calculation of the ground state energy of He-like Fm, Z=100, using a relativistic Sturmian analytic basis set representation for the Coulomb-Dirac Green's function. We have calculated the perturbation theory equivalent of the Dirac-Fock-Breit approximation, and the relativistic correlation energy. Our results agree well with the Grant code, and with calculations of Blundell, Mohr, Johnson, and Sapirstein.

Objectives

For very highly ionized atoms, where the number of electrons is small compared to the nuclear charge, the electrons interact with each other pertubatively. The perturbation theory expansion of atomic energy levels is characterized by the parameters: $a \approx 1/137$, Za, where Z is the nuclear charge, $1/Z$, and $N(N-1)/2\, a$, where N is the number of electrons, as well as quantum numbers. For N small and Z large, this expansion converges rapidly. For high Z, though, Za is not necessarily a good expansion parameter, being $\approx 2/3$ for uranium, so all orders in Za must be included. This can be achieved by complete evaluation of Feynman diagrams. Characteristic diagrams are shown in Figure 1. Our objective is the numerical calculation of these diagrams.

The basic process that enters into the perturbation theory calculations for high-Z atoms, in which the electrons are relativistic, is the interaction of a pair of electrons through a photon. The photon interaction includes the Coulomb interaction, Breit interaction, and retardation. All Feynman graphs correspond to sewing together products of the photon exchange graph. The internal lines of the Feynman graphs represent all possible virtual intermediate excited states for the electron. The required sum over all bound states, all

positive energy continuum electron states in the strong Coulomb field from the nucleus, and all the negative energy continuum states of the Dirac sea is implemented with the Green function. The form of the analytic basis set representation[1] enables the matrix elements for photon exchange to be calculated analytically. For high photon frequency (large energy difference between initial and final electron states in the matrix element), the matrix element calculation is very efficient. This regime is the most difficult for purely numerical schemes.
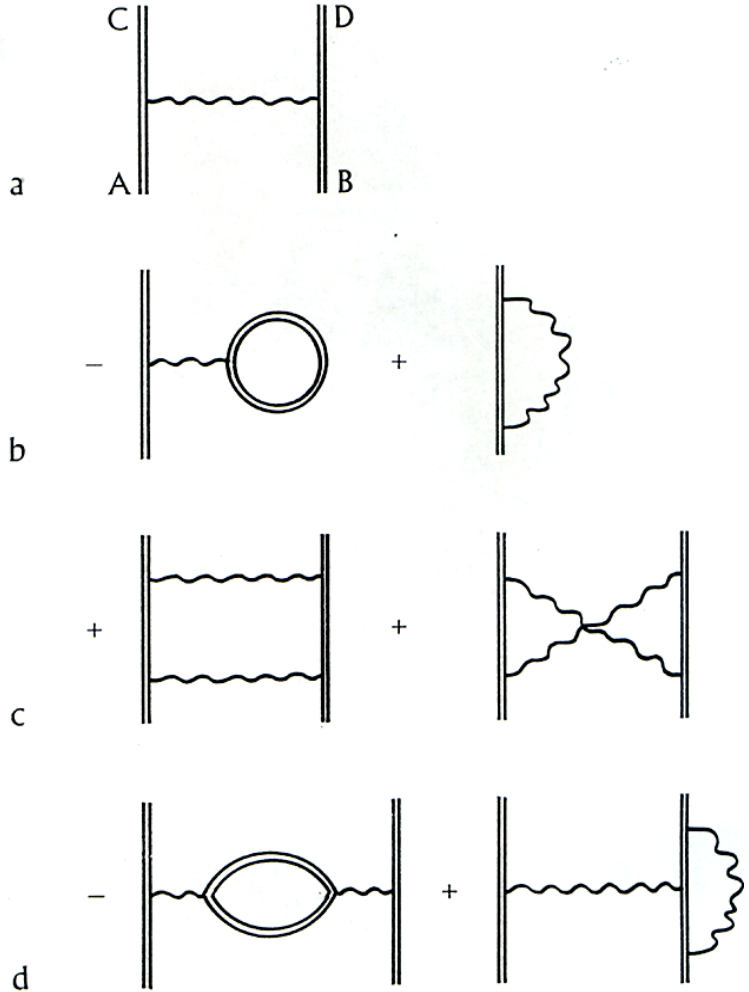
Figure 1. Typical Feynman diagrams for the calculation of atomic energy levels of high-Z He-like ions: (a) Photon exchange diagram representing the interaction of electrons in quantum states A, B→C, D; (b) Vacuum polarization and self-energy processes contributing to the Lamb shift; (c) Correlation ladder and crossed photon ladder; and (d) radiative corrections to photon exchange (screening of the Lamb shift).

In FY95 we implemented the calculation of the correlation energy graphs, the photon ladder box graph, and the crossed-photon box graph. The calculation involves an integration over photon frequency, which is done by contour rotation in the complex plane. There are pole contributions and a principal value integral contribution. The pole terms contribute to the Dirac-Fock-Breit approximation. Along with the single photon exchange energy and the Dirac energy of two hydrogenic electrons, the results[2] for Z=100 are: $E_{gs}(Z=100)$=–11878.38844+92.238001–(0.210982+0.168834+0.005665)=–11780.53825 a.u. The terms in parentheses refer to the natural separation of the pole term's exchanged photons into Coulomb-Coulomb (C-C), Coulomb-Breit (C-B), and Breit-Breit (B-B) contributions. Higher terms in this series are smaller by powers of $1/Z$. This number agrees with the Grant code run in the Dirac-Fock-Breit approximation for point nucleus to the expected accuracy. The principal value integral contribution of the box graphs gives the correlation energy. For the relativistic Coulomb correlation, which is only part of the content of this graph, we get (only a finite sum of the partial wave series),ΔE_C=–0.0677 a.u. This number is usually combined with the Coulomb pole contribution to give $E^{(2)}$= –0.2787 a.u. This result agrees well with the result of Blundell, Mohr, Johnson, and Sapirstein,[3] $E^{(2)}$=–0.27690 a.u., when account is taken of finite nuclear size (which reduces the magnitude of the point nucleus number). These results demonstrate the viability of this calculational scheme for high-Z QED Feynman graphs. In FY96, we will continue the evaluation of the remaining graphs of Figure 1 for the ground state and excited states of He-like ions.

References

1. N. L. Manakov and S. A. Zapryagaev, "Coulomb Green's function of the Dirac equation and calculations with stationary perturbation theory," *Sov. J. Nucl. Phys.* **23**, p. 482, 1976.

2. D. J. Hylton and N. J. Snyderman, "Analytic basis set for high-Z atomic QED calculations: He-like ions," UCRL-JC-122418, LLNL, Livermore, CA, submitted to Phys. Rev. A.

3. S. A. Blundell, P. J. Mohr, W. R. Johnson, and J. Sapirstein, "Evaluation of two-photon exchange graphs for highly charged heliumlike ions," Phys. Rev. A **48**, p. 2615, 1976.

Investigation of Organic Nonlinear Optical Crystals for Harmonic Frequency Conversion and Electro-Optics

Principal Investigators: Ravindra B. Lal (Alabama A&M University) and Howard W. H. Lee (LLNL)
LLNL Collaborator: J. Diane Cooke

Abstract

Organic materials have emerged in recent years as the leading choice of materials for optoelectronic and photonic applications. This attention stems from their remarkable optical, chemical, and structural properties, along with their easier processing. Organic materials can exhibit large optical nonlinearities, high optical damage thresholds, and broad spectral transparency ranges. They can also be conveniently processed to give high optical quality surfaces; can be made into thin films, waveguides, or bulk structures; and can be used to fabricate unique layered, thin film structures with different optical properties within each layer. We conducted a detailed investigation of the nonlinear optical properties of organic crystals grown with a novel solution growth technique at the Department of Physics at Alabama A&M University (AAMU). Our studies included the characterization of nonlinear optical properties and damage thresholds of crystals for high power laser applications, and will include the fabrication of possible devices enabled by these crystals, such as harmonic frequency converters, electro-optic switches, and modulators.

Objectives

Our research involves the development of new organic materials for applications in nonlinear optics, optoelectronics and photonics, and sensors. Specifically, we intend to:

- Develop, synthesize, and grow new organic-based optical materials for nonlinear optical and optoelectronic applications.
- Investigate and characterize the optical properties of these systems (second and third order nonlinear optical effects, spectral transparency, excited state dynamics, optical damage properties).

- Design and incorporate these new materials into optoelectronic devices and sensors (frequency converters, modulators, switches, waveguide structures, LEDs, flat panel displays, etc.).
- Theoretically model and guide experimental research on these organic systems.

AAMU has extensive synthetic and growth facilities to fabricate these organic materials. LLNL has state-of-the-art facilities to characterize the optical, electronic, nonlinear optical, and sensor properties of these new materials, as well as fabrication facilities to incorporate these materials into devices. The strength of this effort derives from the synergism between material synthesis and growth expertise of AAMU, and characterization, modeling, and fabrication capabilities of LLNL.

Progress

Four organic nonlinear optical crystals grown at AAMU were brought to LLNL for optical studies. These crystals are: Mixed methyl-(2,4-dinitrophenyl)-aminopropanoate (MAP:2-methyl-4-nitroaniline [MNA]); 3-methoxy-4-hydroxy-benzaldehyde (MHBA); 4-aminobenzophenone (ABP); and N-(4-nitrophenyl)-(L)-prolinol (NPP). All of these crystals were grown at AAMU by a novel, modified solution crystal growth technique.[1]

All crystals were cut in the proper orientation for optical absorption and frequency doubling studies using a diamond wire saw. These crystals were polished using proper solvents to flat plates of thickness ranging from 2–3 mm.

Optical absorption data were taken on all four crystals using a CARY 5 UV-VIS-NIR dual-beam spectrophotometer between 400–1500 nm. The results are shown in Figure 1 for MHBA, MAP:MNA, ABP, and NPP crystals. The data are consistent with the frequency doubling observed for these crystals. Frequency doubling measurements were made using a Nd:YAG laser and a Ti:Sapphire regenerative amplifier operating at approximately 150 fs and 0.7 mJ/pulse. The output of this laser was focused into a 0.25" thick fused silica substrate to generate a white-light continuum. The three wavelengths used (850 nm, 950 nm, and 1064 nm) were selected from this continuum using appropriate bandpass filters. All crystals gave efficiencies ranging from 4–10%, with ABP giving the highest

efficiency of approximately 10%. These are preliminary results and depend greatly on the optical quality of the crystals. These results could be enhanced by improved growth and polishing techniques of the crystals.

A unique and sensitive, single-beam experimental technique to accurately measure the third-order optical nonlinearity was developed and implemented.[2] Measurements on these organic nonlinear crystals will be carried out with this setup during the academic year.

Measurements of the laser damage thresholds of these crystals conducted at the indicated wavelengths gave threshold values of 1-2 GW/cm^2. These values are comparable to those measured in inorganic crystals and dispel the misconception that organic crystals are particularly susceptible to laser damage. These studies will continue during the academic year.
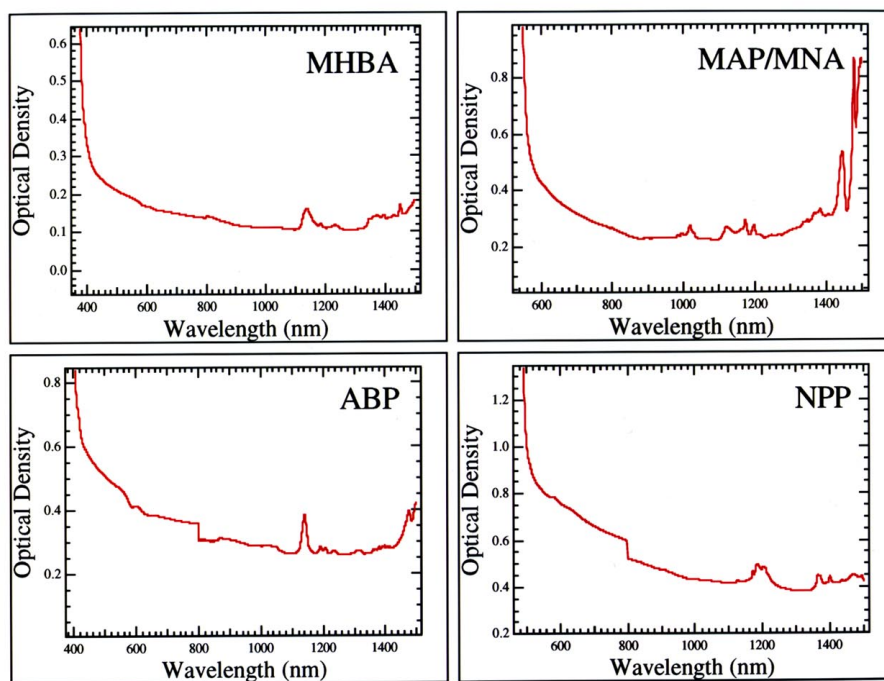
Figure 1

Figure 1. Absorption spectra for organic nonlinear optical crystals investigated in this study.

References

1. H. W. Zhang, A. K. Batra, and R. B. Lal, "Growth of Large MNA:MAP Crystals for Nonlinear Optical Applications," *J. Cryst. Growth* **137**, p. 141, 1994.

2. H. W. H. Lee and R. S. Hughes, Jr., "Anti-resonant Ring Interferometric Nonlinear Spectroscopy for Nonlinear Optical Measurements," *Optics Letters* **19**, p. 1708, 1994.

Studies in High Energy Density Plasmas and X-ray Fluorescence of Condensed Matter

Principal Investigators: Araya Asfaw and Lewis Klein
(Howard University) and Richard Lee (LLNL)
LLNL Collaborator: Ronnie Shepherd

Abstract

Research in the area of high energy density physics was performed at the Lawrence Livermore National Laboratory (LLNL) Nova laser facility and at the Ultra-Short Pulse (USP) laser facility in collaboration with scientists from LLNL, Howard University, Université de Provence, and Oxford University. Work in the area of soft x-ray fluorescence of condensed matter was performed at the Advanced Light Source (ALS) at Lawrence Berkeley National Laboratory (LBNL) in collaboration with scientists from LLNL, LBNL, IBM, NIST, Tulane University, and the University of Tennessee. Our involvement in these activities is supported by the LLNL Research Collaborations Program for Historically Black Colleges and Universities.

Objectives

The research performed in high energy density physics is relevant to plasma spectroscopy and hydrodynamics. Our experiments involve measurement of near megabar shock fronts in crystals by x-ray diffraction, time resolved temperature of radiatively heated tamped foils by x-ray absorption spectroscopy, ion dynamics and redistribution, femtosecond laser pulse soft x-ray conversion mechanisms, and spectroscopic diagnostics of implosion dynamics.

The work in condensed matter physics done at the ALS at LBNL utilizes the brightest third-generation synchrotron light source to map out the localized density of states through transitions between the valence and the core level. This map is modified by the dipole selection rule, and one obtains a selected density of states of one of the elements in the compound of interest.

Progress

Measurement of Shock Fronts in Crystals

A highly uniform near megabar shock can be created in a crystal by laser-irradiating a target to produce soft x-ray radiation, which can be used to drive the shock whereby the front thickness can be examined dynamically by x-ray diffraction. The x-ray heats the layers of the crystal, and ablation produces a uniform shock. X-ray diffraction can then be used to measure the shock front thickness from the shock compressed crystal. The temporally resolved data obtained from such measurements yields information about the optical, mechanical, and electrical properties of the material in the high pressure regime, which cannot be obtained by static measurements.

Five laser beams of Nova are focused into a one millimeter diameter spot and onto a 2000 Å thick free-standing gold foil. A 2-nanosecond square laser pulse with ten kilojoules of energy from the Nd:glass laser at 0.35 µm is used to irradiate the foil. About 10% of the laser light is converted into soft x-rays. The x-rays from the backside of the gold foil volumetrically heat the front layer of a silicon (111) crystal. About 95% of the x-rays from the gold foil is absorbed within 5 µm of the crystal depth, raising the crystal temperature to 15 eV and generating pressures on the order of half a megabar within the first 2 µm depths of the crystal. The shock takes about 4 nanoseconds to traverse the crystal thickness, which is 40 µm. When the shock is within two or three absorption depths of the rear surface, another Nova beam is used to create a vanadium plasma. The helium-like vanadium resonance line is diffracted from the rear side of the crystal onto a temporally resolved x-ray streak camera.

Temporal temperature measurements were made of heated, tamped foils. A 1500 Å MgO foil tamped on both sides with 1000 Å paralyene was heated by soft x-rays generated from a 1500 Å gold foil irradiated with one of the Nova laser beams. A second Nova beam irradiated the front surface of a uranium foil and backlit the MgO plasma to provide a time-resolved K-shell absorption spectrum over the duration of the heating process. Although the spectra obtained from the experiment are in disagreement with hydrodynamic simulation of the x-ray heating process, it consistently shows significant absorption from higher ionization stages associated with higher plasma temperatures than predicted.

Measurement of Femtosecond Laser Pulse Soft X-ray Conversion

The conversion efficiency of a femtosecond laser pulse to soft x-ray conversion in the neighborhood of 50 to 150 Å is measured at the Ultra Short Pulse laser facility of LLNL. The measured conversion efficiency varies from low Z (aluminum) to medium Z (germanium) and high Z (gold). It also depends on the surface finishes (e.g., flat and porous). The results are modeled with hydrodynamic simulations to provide insight into the various mechanisms contributing to the resulting emissivities.

Spectroscopy of Implosion Plasma Dynamics

The plasma dynamics are studied for several fill gases with a trace amount of argon. By analyzing the Ar $1s^2$–$1s3p$ (^1P) line profile, the evolution of the plasma density and temperature as a function of fill gas is examined. The Nova 10-beam laser at LLNL is used to indirectly drive the implosion of a gas-filled plastic microsphere contained in a gold holhraum. The dynamical density measurement is derived from a streak camera line width measurement, and from comparison, with the computed profile. The calculations show that, in certain cases, there is a substantial ion dynamic effect on the line shape. Calculations based on the Frequency Fluctuation Model and comparison with the experimental data provide evidence that ion dynamics may affect the line shape. This study provides a method of obtaining improved understanding of the basic processes in plasma physics of matter compressed to a state of high energy density.

Measurement of Soft X-ray Fluorescence of Condensed Matter

The Ca $L_{2,3}$ and Si $L_{2,3}$ fluorescence spectra of $CaSi_2$ and CaSi were studied. Soft x-rays from undulator beamline 8.0 at the Advanced Light Source of LBNL are monochromatized to excite the samples mounted in the UHV sample chamber. The photons emitted from the sample are detected with a position-sensitive area detector mounted on a 5-meter Rowland spectrometer. These spectra provide s and d partial density of states (PDOS) information for the Ca and Si atoms. The measurements are in good agreement with calculations. In CaSi, inelastic Raman peaks are also observed.
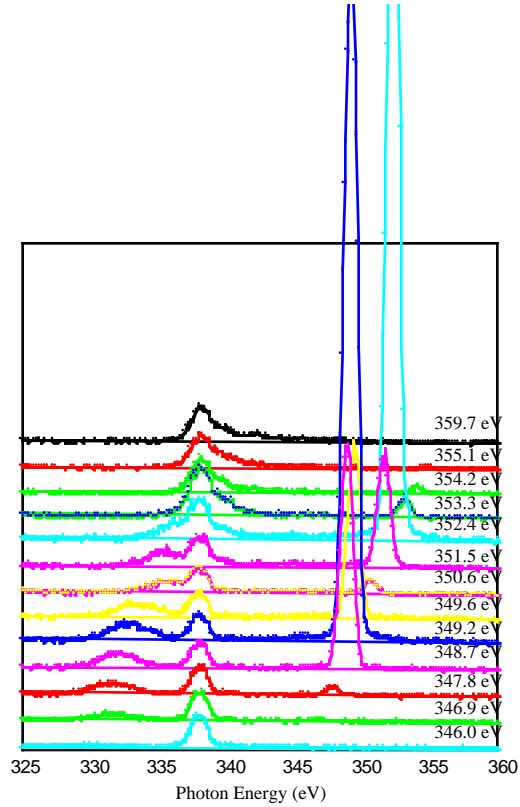
Figure 1. The spectrum of CaSi probed with various excitation energies near the Ca $L_{2,3}$ edge. Raman scattering of soft x-rays is also observed in hexagonal boron nitride using monochromatic x-rays just below the boron K edge. The inelastic features track with the excitation energy and go through resonance as the excitation photon is tuned above the 1s excitation energy of boron, and evolve into normal fluorescence as the excitation energy is raised above the energy needed to excite the boron 1s electron into the conduction band. The inelastic energy loss is identified as an excitation of valence σ electrons into the π^* valence excitation state. Transitions are also observed at and above resonance $\pi-\pi^*$. The existence of a side band on the elastic peak at resonance also provides evidence of additional electronic and phonon loss processes. Similar results also have been observed for B_2O_3.
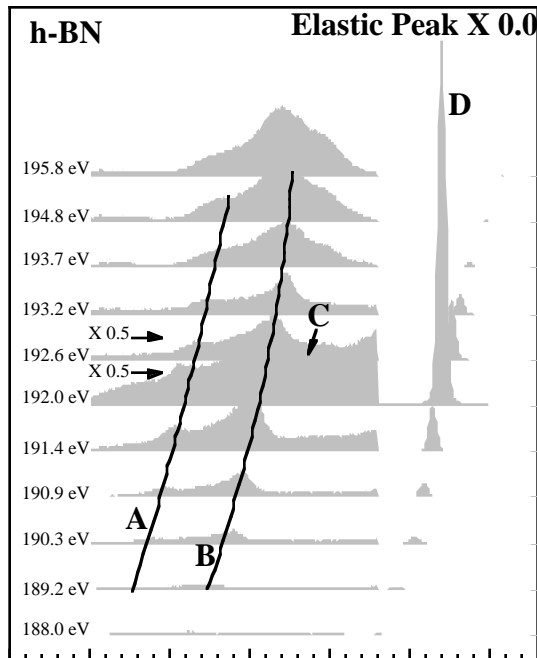
Figure 2. The boron K soft x-ray fluorescence spectra of h-BN for excitation
near threshold. For all excitation energy below the resonance energy
(192 eV), the inelastic spectrum shows two peaks (A and B) separated by
5 eV, and a much more intense elastic peak (D) at higher energy. The
inelastic spectra track the excitation energy, so that the upper peak (B)
maintains a constant separation of 11 eV below D. At the resonance energy,
a new feature (C) appears in the inelastic spectrum and disappears as the
excitation energy is increased at about 2.5 eV above B. At high energies,
C disappears as the excitation moves off resonance and reappears as part of
the normal fluorescence spectrum.

References

1. A. Koch, C. A. Back, C. A. Iglesias, D. L. McWilliams, R. C. Cauble, E. J. Hsieh, N. Kornblum, N. C. Woolsey, J. C. Moreno, A. Asfaw, J. K. Nash, F. J. Rogers, and R. W. Lee, "Time-Resolved Temperature Measurements of Radiatively Heated Tamped MgO Foils by Ka Absorption Spectroscopy," *JQSRT* **54**, No. 1/2, pp. 227–236, 1995.

2. C. Mosse, A. Calisti, R. Stamm, B. Talin, J. Koch, A. Asfaw, N. Woolsey, C. Back, R. Lee, J. Seeley, and L. Klein, "X-ray Laser Photopumped Resonance Fluorescence," Submitted to *Phys. Rev. E.*

3. N. Woolsey, A. Asfaw, B. Hammel, C. Keane, C. Back, R. Lee, A. Calisti, C. Mosse, R. Stamm, B. Talin, J. Wark, and L. Klein, "Spectroscopic Study of Compressed High Energy Density Matter," submitted to *Phys. Rev. E.*

4. R. Sheperd, A. Asfaw, D. Price, M. Foord, R. Walling, and R. Lee, "The Measurement of Sub-picosecond Laser Pulse X-Ray Conversion Mechanisms," to be submitted to *Phys. Rev. Lett.*

5. J. Jia, T. A. Callcott, A. Asfaw, J. A. Carlisle, L. J. Terminello, D. L. Ederer, and R. C. C. Perera, "Occupied Electronic States of $CaSi_2$ and CaSi: Soft X-ray Fluorescence Spectroscopy," *Phys. Rev. E* **15**, 1995.

6. J. Jia, T. A. Callcott, A. Asfaw, J. A. Carlisle, L. J. Terminello, D. L. Ederer, F. J. Himpsel, and R. C. C. Perera, "X-ray Raman Scattering in h-BN Observed by Soft X-Ray Fluorescence Spectroscopy," submitted to *Phys. Rev. Lett*.

7. J. Jia, T. A. Callcott, A. Asfaw, D. L. Ederer, R. C. C. Perera, J. A. Carlisle, L. J. Terminello, and F. J. Himpsel, "Resonant Inelastic Raman Scattering Observed near B K edge in h-BN and B_2O_3 by Soft X-ray Fluorescence Spectroscopy", *APS* **40**, No. 1, p. 337, March 1995.

8. J. Jimenez-Mier, D. L. Ederer, U. Diebold, T. A. Callcott, L. Zhou, J. J. Jia, J. Carlisle, E. Hudson, L. J. Terminello, A. Asfaw, F. J. Himpsel, and R. C. C. Perera, "Stoichiometric-Dependent Inelastic and Resonant Scattering in Titanium and Its Oxides," *APS* **40**, No. 1, p. 389, March 1995.

9. L. Zhou, T. A. Callcott, J. Jia, A. Asfaw, D. L. Ederer, R. C. C. Perera, "The Sulfur $L_{2,3}$ Emission Spectra of TM-S Compounds," *APS* **40**, No. 1, p. 841, March 1995.

10. N. C. Woolsey, A. Asfaw, R. W. Lee, J. S. Wark, and R. Cauble, "Measurement of Near M-bar Shock Fronts in Crystals by X-ray Diffraction," APS Topical Conference on Shock Compression of Condensed Matter **40**, No. 6, July 1995.

11. N. C. Woolsey, R. W. Lee, A. Asfaw, C. A. Back, S. Glenzer, B. Hammel, D. Kalantar, J. Koch, J. Moreno, L. Klein, B. Talin, R. Stamm, L. Godbert, and C. Mosse, "Spectroscopy of argon-doped indirectly driven ICF capsules," APS 37th Annual Meeting of the Division of Plasma Physics **40**, No. 11, p. 1670.

12. A. Asfaw, R. Sheperd, R. Lee, J. Koch, and N. Woolsey, "Time Resolved Soft X-ray Measurement from Femtosecond Laser Plasma," APS 37th Annual Meeting of the Division of Plasma Physics **40**, No. 11, p. 1722.

13. A. Asfaw, C. Back, T. Barbee, L. Da Silva, S. Glenzer, L. Klein, R. Lee, J. Moreno, A. Wan, N. Woolsey, C. Mosse, B. Talin, R. Stamm, A. Calisti, and J. Koch, "Photopumping and Redistribution in Laser-Produced Plasma," APS 37th Annual Meeting of the Division of Plasma Physics **40**, No. 11, p. 1724.

14. R. Shepherd, A. Asfaw, J. Koch, R. Lee, D. Price, B. Young, A. Osterheld, M. Foord, R. More, and R. Stewart, "Sub-kilovolt, broadened x-ray emission from short pulse laser-produced plasma at the Lawrence Livermore National Laboratory Ultra Short Pulse Laser," APS 37th Annual Meeting of the Division of Plasma Physics **40**, No. 11, p. 1661.

15.   N. C. Woolsey, A. Asfaw, C. A. Back, R. Cauble, S. Glenzer, E. Hsieh, J. S. Wark, and R. W. Lee, "Strain Measurements of Shock Compressed Solids at the Lattice Scale," APS 37th Annual Meeting of the Division of Plasma Physics **40**, No. 11, p. 1854.

Studies in High Energy Density Plasmas

Principal Investigators: Lewis Klein (Howard University) and
Richard Lee (LLNL)
LLNL Collaborators: Ronnie Shepherd and Richard Ward
Students: Daniel Felten and Aaron Roane

Abstract

*The work performed in the area of high energy density science relevant
to plasma spectroscopy and hydrodynamics has been ongoing in a broad
collaboration between Howard University and LLNL. Further, participants
from Université de Provence in Marseille and Oxford University have also
become involved in this work. There has been substantial progress in the
development of plasma diagnostic techniques and the study of heat
propagation in laser irradiated targets.*

Objectives

The research performed under this contract is related to an
ongoing experimental program at the Livermore Nova laser facility
and utilizes the unique experimental potential of the ICF lasers. The
energy densities and specific energies achievable with the ICF source
are in an interesting high energy density regime, which is not possible
with high explosive. These experiments are of particular current
interest because of their relevance to a large number of problems in
the formation of hot dense matter. In addition, for diagnostic
purposes, studies have been made of the spectral profiles of the
radiation emitted from the high energy density matter created in
laser implosion investigations.

Progress

Outlined below are three areas in which substantial progress
has been made. First, a method for calculating the redistribution of
resonance radiation in hot, dense plasmas has been developed by
extending the Frequency Fluctuation Model (FFM).[1] The FFM is
based on a numerical technique that replaces the primitive
inhomogeneous Stark component contributions to the linear response
line shape with the observable radiative channels. A comparison with
standard approximate redistribution functions is presented, and

experimental tests of the theory are also suggested. Second, we will briefly review the experimental and theoretical work on the propagation of energy into underdense foam targets irradiated by a laser. Third, a theoretical and experimental time-resolved spectroscopic investigation of indirectly driven microsphere implosions is described. The plasma dynamics is studied for several fill gases with a trace amount of argon. Calculations demonstrate that, in certain cases, there can be a substantial ion dynamics effect on the line shape. The FFM is used to compute the effect on the line profile, and a comparison with the experimental spectra provides evidence that ion dynamics may be affecting the line shape. This study provides a method for obtaining improved understanding of the basic processes dominating the underlying plasma physics of matter compressed to a state of high energy density.

Development of a Spectral Line Model to Handle Ion Dynamics and Redistribution

Recent advances in the computation of the radiative properties of complex ions in hot, dense plasmas, made possible by the development of the Frequency Fluctuation Model (FFM) developed in this effort in collaboration with the University of Provence, have resulted in an adequate understanding of the effect of the plasma environment on the emission or absorption process and the shape of the associated spectral lines.[2] In addition, the FFM treatment of ion field fluctuations has resulted in calculations that provide a good diagnostic of the plasma parameters under a wide range of conditions.[3] However, for plasma lines with a large optical depth, there remain difficult problems concerning radiative transfer, which are not simply related to calculations of the one-photon absorption or emission spectrum. The development of a computational ability to treat the scattering of near-resonant radiation in hot, dense plasmas requires a theoretical formulation of two photon plasma spectral properties in the presence of a combination of homogeneous and inhomogeneous processes. In the following, the usual linear response calculations of the spectral line shape will be extended to the higher order absorption and re-emission response function that is required for the computation of radiation redistribution.

A particular motivation for these calculations can be found in a possible experimental application arising from recent progress in the development of X-ray lasers with wavelengths appropriate for photo-pumping the ground-state transitions of multi-electron ions.[4] These lasers have sufficient brightness such that they could be suitable for use as resonant photo-excitation sources[5] in pump-fluorescence experiments designed to study radiative transfer in hot, dense plasmas. The spectroscopic data resulting from these photopumping experiments should be a significant improvement over the first observations of photopumping in high-Z plasmas, which were limited to the measurement of the total, integrated resonance fluorescence.[6] The pumping technique utilized in those experiments involved a hot, laser-produced aluminum plasma that pumped a significant population of ground-state He-like ions in another, spatially distinct, but more dense, aluminum plasma. A more detailed set of experiments, which completely characterized the fluorescence lines, was carried out later on this same system[7] and radiative transfer effects were studied using a numerical simulation.[8] However, a complete study of radiative redistribution in these high-Z plasma experiments was not possible with the available spectral resolution and pump intensity.

For the photopumping experiment of interest here, the narrow bandwidth and large pump intensity of the monochromatic X-ray laser can be used to resolve most of the problems associated with the detailed spectral observation of the redistributed fluorescence produced by the photopumping. The accurate measurement of the radiative redistribution function near the emitter resonance also should become feasible. Comparison of the experimental results with the model calculations, to be described, could also lead to a better understanding of the kinetic processes affecting the propagation of radiation in these complex systems. Estimates of the effect of pumping with a near-resonant X-ray laser indicate that significant perturbations of the ionic emitter population kinetics could result[4] so that the experiments, therefore, will be an important source of detailed dynamical information on the processes involved in radiative redistribution.

Because current X-ray lasers are not tunable, a search for ionic transitions that have a near resonance with specific laser wavelengths has been performed. For the yttrium 155Å X-ray laser line, which is particularly intense, a number of candidate transitions were

identified. Measurements made of the laser detuning from the 4f-3d transitions of H-like Na and He-like Mg enabled a precise determination of the laser line wavelength. However, the fluorescence spectrum was too weak to be observed in these experiments. This was because the plasma temperature was a substantial fraction of the transition energy, which then gives rise to a small population difference between the two states involved. For this reason, experiments are proposed in the following that involve transitions from the ionic ground state in relatively cool plasmas. These experiments can be expected to yield more intense fluorescence signals, which could be more strongly affected by redistribution processes. Using published transition wavelengths,[9] one of the 3d-2p lines of fluorine-like magnesium, which at 146.5260Å is separated by only 11 mÅ from the zirconium 146.515Å X-ray laser line, has been identified as a possible candidate for an experiment. Another possibility is the 3d-2p F-like Mg line at 140.4250Å, since it is detuned by only 5 mÅ from the 140.430Å niobium X-ray laser line.

As an example of the fluorescence spectrum calculated, we present the redistribution function of fluorine-like magnesium (MgIV) pumped near the $(2p)^4 3d-(2p)^5$ fine structure lines that are in the vicinity of the 140.430Å niobium laser line. Ten fine structure transitions in this range are included in the computation. A particularly strong transition is at 140.425Å and is detuned by only 5mÅ from the laser line. In Figure 1, the calculated absorption line profile for the 3d-2p transition of F-like Mg, centered at 140 Å, of the F-like Mg ion, is presented for plasma conditions of low electron density, $N_e = 10^{20}$cm^{-3}.

Because of the narrow widths due to electron collisional broadening at this density, the various fine structure lines included in the calculation can be seen. The fine structure components of the ion lines have been measured[10] to an accuracy of 1mÅ, but the uncertainty in the absolute wavelength of the laser could be as large as 50mÅ. To exhibit the effect of laser detuning on the fluorescence spectrum, we shall study the redistributed emission as a function of laser detuning.

The redistribution function for the Mg IV 3d-2p transition in a plasma with temperature, T=100eV, and electron density, $N_e = 10^{21}$cm^{-3}, has been computed, and Figure 2 illustrates the $R(\omega_L, \omega_S)$ surface for this case. The absorption line shape is presented

Figure 1. The calculated absorption lineshape function of the Fluorine-like Mg 3d-2p transition. The electron density in the plasma is $N_e = 10^{20}$ cm^{-3} and the temperature is $T_e = 100$ eV. For these plasma conditions, the electron collision broadening is sufficiently small that individual fine structure and Stark components are resolved.
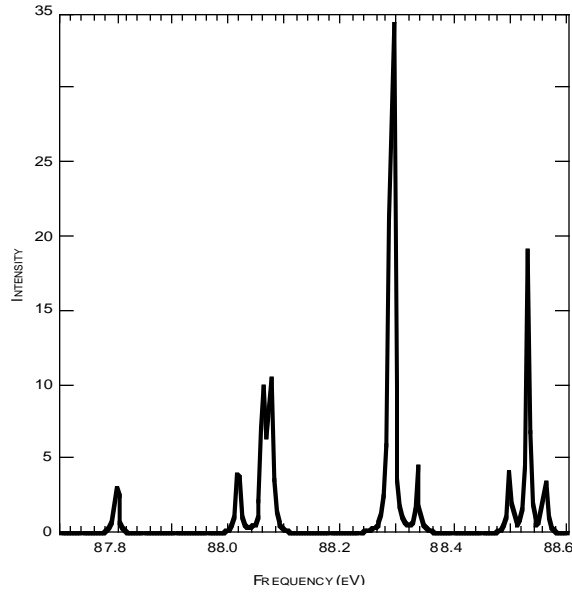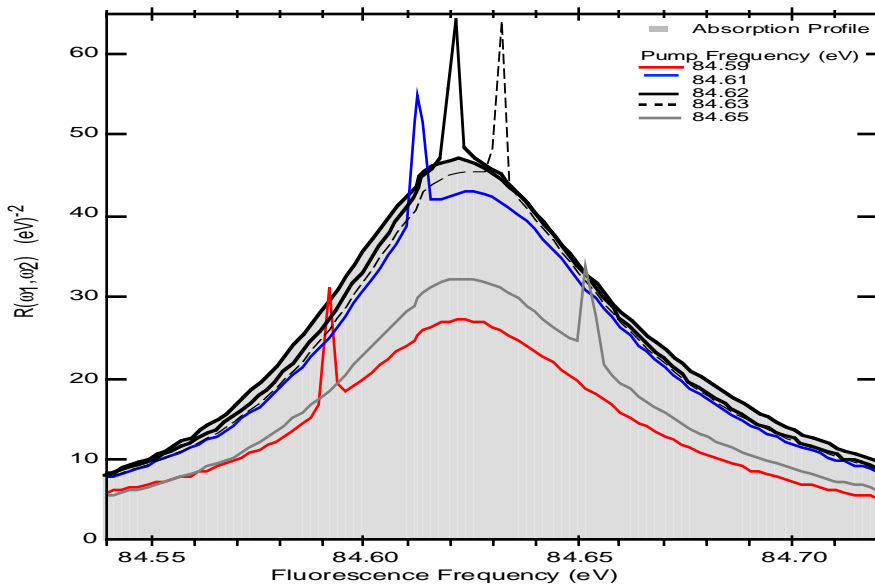

Figure 2. The calculated absorption lineshape function of the Fluorine-like Magnesium 3d-2p transition. The electron density in the plasma is $N_e = 10^{20}$ cm^{-3}, and the temperature i, $T_e = 100$ eV. For these plasma conditions, the electron collision broadening is sufficiently small that individual fine structure and Stark components are resolved.

at the rear plane for comparison with the redistributed fluorescence. The ion Stark broadening is negligible for these plasma conditions, but the electron collision broadening has caused the merging of the fine structure pattern so that only a few distinct resonances remain. Inelastic collisions, which could mix the fine structure components, have not been accounted for in the calculations, so no redistribution between these elements is included. Therefore, the fluorescence spectrum illustrated in Figure 2 originates primarily from the pumping of independent fine structure components. For pump frequencies not too far from resonances, this gives rise to complete redistribution for each component separately. That is, since there is no mixing of the components by inelastic collisions in the calculation, near resonant pumping of each homogeneous component can only redistribute the fluorescence within the same component. However, off resonant pumping, as will be seen, will yield a fluorescence spectrum that is shared among neighboring components and has a significant coherent, or Rayleigh, line. This is illustrated in Figure 3, where pump frequency sections through the surface of Figure 2 are plotted.

The redistribution spectrum calculated with the pump frequency near the central feature of the absorption line shape (the dashed line in Figure 3) can be seen to closely approximate the absorption line shape of the central peak and represents the narrow pump case, or complete redistribution for this component. The fluorescence profile, therefore, resembles R_{III} for this one component. Pumping near a given resonance gives rise to a fluorescence spectral shape that is the same as that of the corresponding resonance of the absorption profile; however, for
non-resonant pumping, this is no longer the case. The fluorescence spectrum has the characteristics of partial redistribution whenever the pump frequency is in the wing of the components. This is seen in the shape of the fluorescence spectrum created by an off-resonant pump frequency and is represented by the solid line profile in Figure 3.

The spectral shape can be seen to be completely different from the absorption line for pumping in this frequency region. The Rayleigh scattering, which is seen at the pump frequency, is the central peak, and the two side resonances are the redistribution of pump radiation to the two adjacent components of the absorption line. As the pump frequency moves further toward the higher frequency resonance, the

fluorescence line shape again represents complete redistribution for this component, as can be seen in the profile outlined by the light gray line in Figure 3.

Propagation of Energy in Laser Irradiated Foams

The results of experiments in which a high power laser is used to irradiate low density (4–9 mg/cc) silica aerogel and agar foam targets have been pursued to understand the coupling of energy into underdense material. The solid interaction and energy transport through the material were monitored with time-resolved imaging diagnostics, and the data show the production and propagation of an x-ray emission front in the plasma. The emission-front trajectory data are found to be in significant disagreement with detailed simulations, which predict a much more rapid heating of the cold material. The data suggest that this discrepancy is not explainable by target
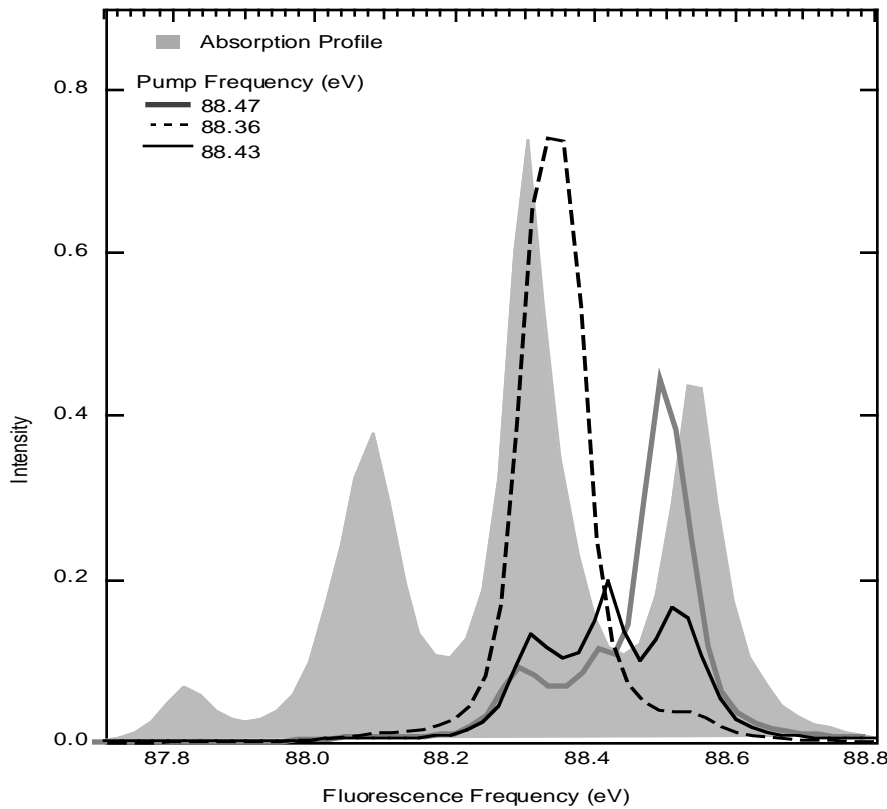
Figure 3. The calculated radiative redistribution function with three different pump frequencies for the Fluorine-like Magnesium 3d-2 transition: $N_e = 10^{21}$ cm^{-3} and $T_e = 100$ eV.

inhomogeneities. Further, the evidence suggests that energy transport into the cold material be dominated by thermal conduction; however, no completely satisfactory explanation for the discrepancies is identified, and further experimental and theoretical research is necessary to resolve this important problem in laser plasma interaction physics.

Figure 4 is a schematic of the experiment, which shows that the instrumentation is fairly complete and that the side-on images of the emission front can be mapped in both space and time. It is these data that represent the critical source for comparison with the heat flow calculated by both detailed simulation and simple hydrodynamic heat flow. In summary, what we find is that the use of a detailed simulation, including the laser plasma coupling, yields a heat front propagation velocity into the foams that is far too rapid. On the other hand, we find that when it is assumed that the laser energy is deposited only at the surface of the foam target, leading to a "hot-plate" model for the heat flow, the correct x-ray emission front velocity is obtained.
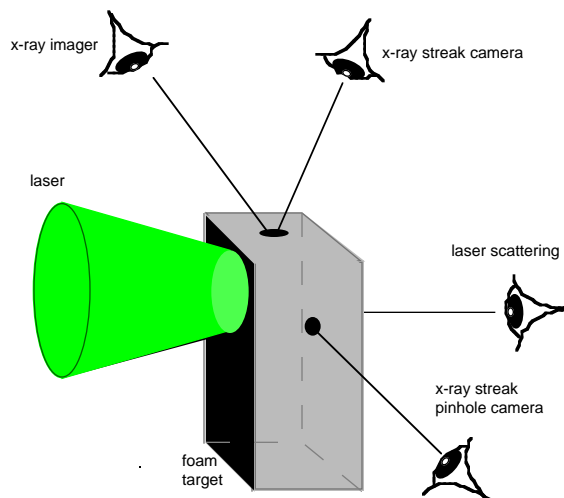
Figure 4. Schematic set up of x-ray emission front measurements.

An example of this is shown in Figure 5. In looking at Figure 5, we see that the emission front data are in significant disagreement with the detailed laser-plasma interaction and hydrodynamics simulations. These data are in qualitative agreement with previous work, but here we have excluded the possibility that the source of the discrepancy is the initial target density inhomogeneities. Instead we find evidence in the experimental data that suggests the energy transport into the cold material may be dominated by electron thermal conduction from a relatively shallow laser energy deposition region, and this is supported by the results of a simple "hot-plate" thermal conduction model.

Even though we find that this model explains most of the features of the data, it does not address the mechanism by which the laser energy might be absorbed over a shallow depth. We can suggest that strong side scattering, strong anomalous absorption and/or compression above the critical density could be responsible. For further information, see the paper that is to be published in *Physics of Plasmas*.[10]

Figure 5. The comparison of the trajectory of the x-ray emission front versus time for low and modest irradiance cases. The black curves are for the modest irradiance and the blue for the low irradiance cases. The dashed lines represent the calculations. Note that the left plot is for the detailed simulation and shows poor agreement, while the right plot is for the simpleheat flow where energy source is constrained to the surface.

Spectroscopic Diagnostic Studies of Implosion Dynamics

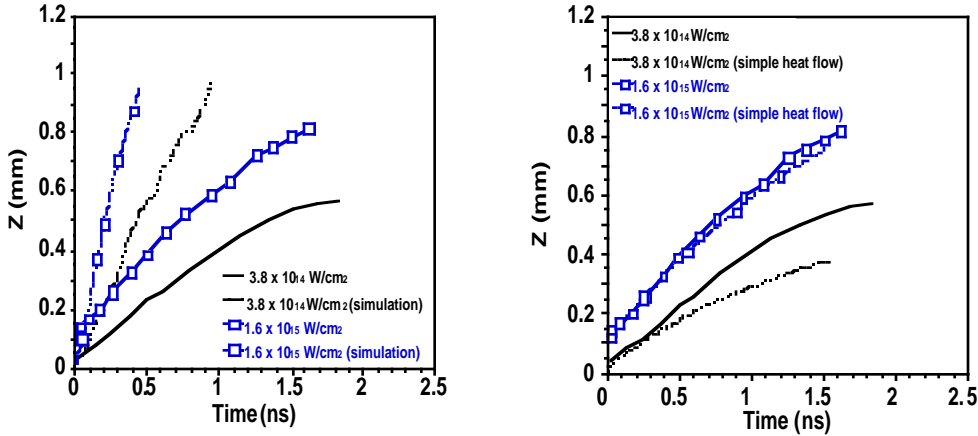The importance to the general program of work of implosions is to provide a plasma environment that achieves high energy density (which is not essential to our studies), but which can be separated from the laser-matter coupling problems. The implosion of microspheres provides such a system insofar as the shock that creates the hot, dense plasma at the core of the implosion is well separated in time and space from the laser-matter interactions. Indeed, the parameterization of the hohlraum drive (called, in ICF parlance, hohlraum characterization) allows the implosion to be studied without recourse to the laser. Thus, so much energy into the laser entrance hole, so much shock pressure, etc. This indicates that we can study the convergence onto the axis of a very strong shock.

With this in mind, we have set out to first reproduce the work we had done previously in the spectroscopic study of Ar-doped deuterium-filled microspheres. Since that worked stopped at the point at which we "measured" the high density at the implosion core, much very fertile ground is left to cover. We have so far made measurement of the Ar and come up to speed. We have further used alternate fills, such as neon, to modify the line shape structure.

The plasma dynamics is studied for several fill gases with a trace amount of argon. Through an analysis of the ArXVII $1s^2$-$1s3p^1P$ line profile, the evolution of the plasma density and temperature as a function of fill gas is examined. The theoretical calculations are performed with the FFM, which has been previously benchmarked through the analysis of specific complex ionic spectra in hot, dense plasmas. The experimental aspect of the work utilizes the LLNL Nova 10-beam laser facility to indirectly drive the implosion of a gas-filled plastic microsphere contained in a gold hohlraum. The dynamical density measurement is derived from a streak camera line width measurement and a comparison with the computed profile. Calculations demonstrate that in certain cases there can be a substantial ion dynamics effect on the line shape. The frequency fluctuation model is used to compute the effect on the line profile, and a comparison with the experimental spectra provides evidence that ion dynamics may be affecting the line shape. This study provides a method for obtaining improved understanding of the basic processes

dominating the underlying plasma physics of matter compressed to a state of high energy density.

As one example of the effort in this area, we discuss the use of different fill gases in the microsphere with the use of the same Ar dopants. The challenge is, therefore, to design a series of implosion experiments, increasing the mean mass of the fill gas but retaining similar implosion dynamics, so that measurements can be made at the same plasma conditions for all fill gases. The effect on the different fill gases can be understood by looking at the change in the ion motion as it effects the emitter. To quantify the ion motion effect, the ion field autocorrelation function has been calculated by a simulation technique for several proposed fill gases under plasma conditions occurring in an imploded core of a microsphere. The autocorrelation function gives a measure of the mean time for ion field changes to occur. When the inverse of the mean time, the mean fluctuation frequency of the ion field, is comparable to the electron fluctuation frequency (roughly, the electron plasma frequency), the static ion approximation fails and ion dynamics must be considered.

In Figure 6, the ion field autocorrelation function, $C_{EE}(t)$, is plotted against time in units of the 70 times the inverse electron plasma
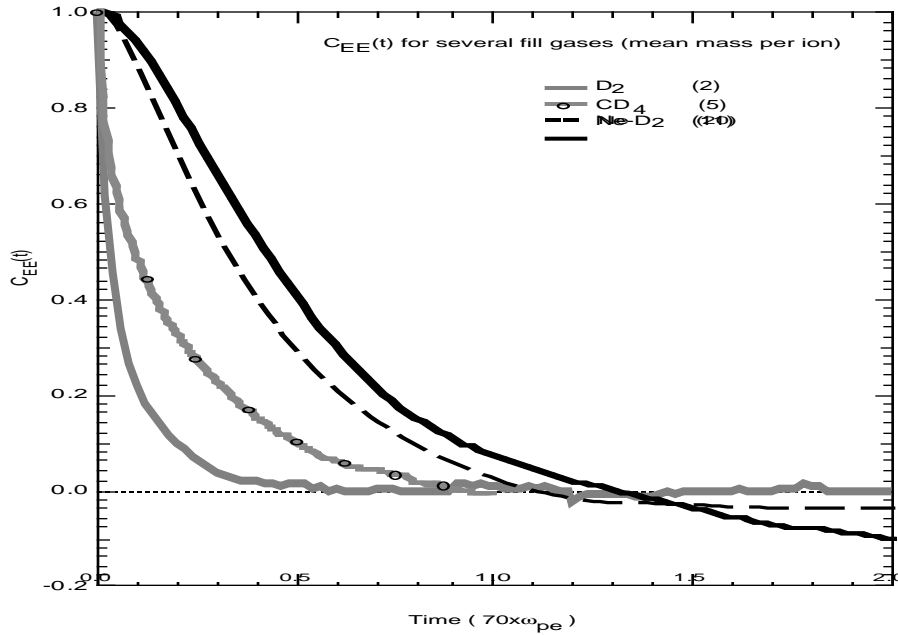

Figure 6. The electric field autocorrelation function for four different fill gases at $N_e = 1.2 \times 10^{24}$ cm^{-3} and $T_e = 1.55$ keV. The abscissa is in units of 70 times the inverse of the electron plasma frequency.

frequency for electron density, 1.2×10^{24} cm^{-3}. The case of deuterium, deuterated methane, a 50/50 mixture of deuterium and neon, and pure neon as fill gases are displayed. An exponential fit to the long time behavior of the autocorrelation function permits the extraction of a mean decay time and, hence, a fluctuation frequency for the different fill gases. Note the rapid decrease in the ion field fluctuation frequency with increasing mean mass of the fill gas.

In fact, by the time the mean mass is that of the 50/50 mixture of neon and deuterium, the dynamics is almost the same as that of pure neon. This decrease in fluctuation frequency is reflected in the ion dynamic effect on the line shape, as can be seen in Figure 7. In this figure, the static ion line shape is compared with the profile calculated with ion dynamics for the indicated fill gases. The central dip almost completely disappears for deuterium, is partially filled in for the methane case, then approaches the static case when neon is the fill gas. It is this effect that is to be verified in order to confirm that ion dynamics is affecting the line shape. That is, by varying the fill gas, we should (if the profile observed represents the intrinsic profile) see the dip in the center of the line when fill gases heavier than D_2 are used.
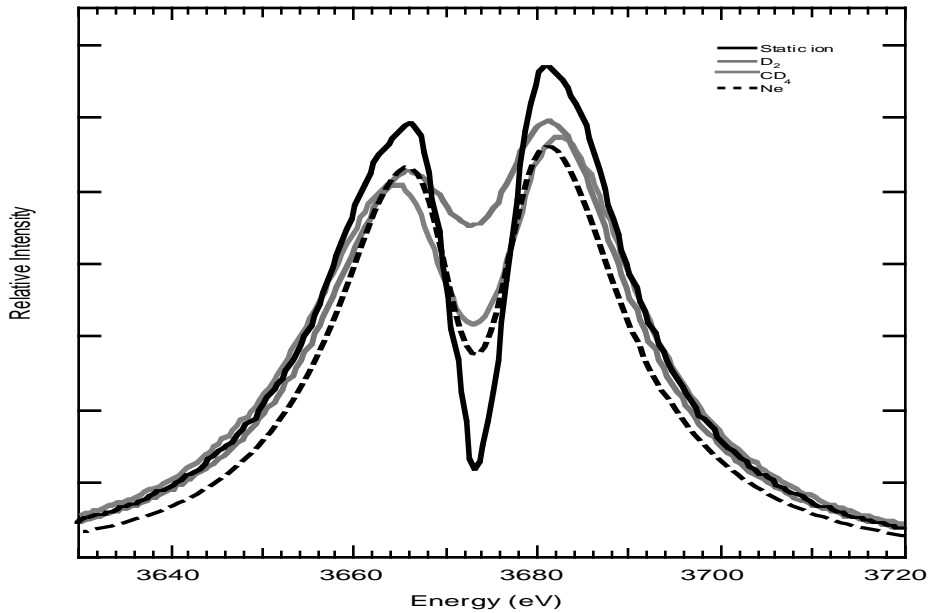

Figure 7. The static ion line shape compared with the profile calculated with ion dynamics for four different fill gases at $N_e = 1.2 \times 10^{24}$ cm^{-3} and $T_e = 1.55$ keV.

In addition to the above study of ion dynamics, spectroscopic computational models have now reached a stage of sophistication that permits very large-level manifolds to be considered in addition to more subtle effects. In this way, the effect of satellite lines on the resonance line profile, as well as ion dynamics, can be considered. These codes have been extensively tested against molecular dynamics simulations and will permit extremely precise plasma diagnostics; this allows us to move forward to the study of detailed kinetics and the effects of radiative transfer on the line formation in high energy density plasmas. For this purpose, a series of experiments have been proposed to measure the implosion dynamics of indirectly driven targets. The experiments discussed will now extend the results obtained earlier with an Ar/D_2 mixture and will provide critical data for the large-scale ion dynamics calculations possible with the FFM codes.

References

1. B. Talin, A. Calisti, L. Godbert, R. Stamm, R. W. Lee, and L. Klein, *Phys. Rev. A* **51**, p. 1918, 1995.

2. A. Calisti, L. Godbert, R. Stamm, and B. Talin, *JQSR* **51**, p. 59, 1994.

3. L. Godbert, A. Calisti, R. Stamm, B. Talin, R. Lee, and L. Klein, *Phys. Rev. E* **49**, 1994, p. 5644. L. Godbert, A. Calisti, R. Stamm, B. Talin, J. Nash, R. Lee L. Klein, S. Glenzer and H.-J. Kunze, *Phys. Rev E* **49**, p. 5889, 1994. Elton, X-Ray Lasers (Academic Press, San Diego, 1990).

4. J. Koch, R. Lee, J. Nilsen, J. Moreno, B. MacGowan, and L. Da Silva, *Appl. Phys B* **58**, p. 7, 1994.

5. C. Back, R. Lee, and C. Chenais-Popovics, *Phys. Rev. Lett.* **63**, p. 1471, 1989.

6. C. Back, C. Chenais-Popovics, and R. Lee, *Phys. Rev. A* **44**, p. 6730, 1991. C. Back, J. Castor, P. Dykema, R. Klein, and R. Lee, *ibid*, p. 6743.

7. Kelly, *J. Phys. Chem. Ref. Data* **16**, Supp. I, 1987.

8. Johannesson, T. Lundstrîm, and L. Minnhagen, *Physica Scripta* **6**, p. 129, 1972.

9. Moreno, J. Nilson, J. Koch, B. MacGowan, J. Scofield, and L. Da Silva, *Appl. Phys. B* **58**, p. 3, 1994.

10. A. Koch, L. Klein, R. W. Lee *et al.,* to be published in *Phys. Plasmas.*

Development of Solid Electrolyte Materials for Gas Phase Sensors and Fuel Cells

Principal Investigators: Rambabu Bobba (Southern University) and Robert S. Glass (LLNL)
LLNL Collaborator: G. Bryan Balazs
Students: Charles LeJune, Jr.; Timothy George; and Vineta Young

Abstract

In the summer of 1994 and the fall of 1995, ac impedance and EXAFS studies of cerium oxide doped with oxides of the rare earth impurities were investigated at LLNL and CAMD (Center for Advanced Microstructures and Devices) to explore their applications as sensor and Solid Oxide Fuel Cells (SOFCs). All of these systems show an increase in the conductivity over undoped ceria, with ceria doped with Gd, Sm, and Y showing the highest values. The conductivity increased with increasing ionic radius of the dopant cation. EXAFS spectra were obtained to understand the precise role the dopant plays in modifying the properties of the oxide and to determine the exact location of the dopant in the host lattice.

The main goal of FY95–96 was to determine the local structural environment of trivalent dopants Gd^{3+}, Sm^{3+}, and Y^3, and thereby establish the reasons for the observed high conductivities. We will also investigate the nature of the defect clustering between oxygen vacancies and trivalent ions with increased concentrations. The compositions are believed to be representative of a concentrated solution. A joint effort with CAMD staff was initiated to analyze the EXAFS spectra of ceria with trivalent rare earth dopants. The principal investigator for this project is also developing a Materials Research Instrumentation Laboratory at Southern University to involve graduate and undergraduate students in applied material science research projects.

Objectives

The primary objective of this project was to develop gas phase sensors and fuel cells using solid electrolyte materials. Solid electrolytes have received increased attention in recent years because

of their excellent suitability as electrical conductivity materials at high temperatures. In this project, we are studying the structure and the ionic conductivity of ceria doped with all naturally occurring rare earth elements to explore the suitability of these materials for the above mentioned applications. The dopant cation size and its effect on the host crystal lattice structure are major factors determining the ionic conductivity of solid electrolytes. In order to understand the precise role the dopant plays in modifying the properties of the oxide, the primary information required is the exact location of the dopant in the host lattice. However, in many systems, obtaining this information has proved to be a difficult problem that cannot be resolved by conventional diffraction techniques. For example, the concentration of the dopant may be very low (less than 1 mol%), the dopant may be indistinguishable from the host (e.g., atoms with similar atomic numbers are not differentiated in the usual X-ray diffraction experiments), the dopant may introduce complex disorder in the lattice, or the material may be amorphous. It is therefore important to employ the Synchrotron Radiation-based experimental technique, EXAFS, to obtain structural information completely. The local structural environments of trivalent impurities in ceria have not been reported so far. It is important to investigate the rare earth ions in ceria with Synchrotron Radiation-based techniques such as EXAFS (Extended X-ray Absorption Fine Structure) and XANES (X-ray Absorption Near Edge Structure).

A collaboration with Southern University, Baton Rouge (SUBR), and the Center for Advanced Microstructures and Devices (CAMD, Baton Rouge) was subsequently established as a part of the LLNL Research Collaborations Program (RCP) for HBCUs. The entire family of rare earth ion-doped ceria samples was prepared at LLNL during the summer of 1995. AC impedance spectra were measured in air with a Princeton Applied Research (PAR) Model 273 potentiostat with PAR M383 software and a solatron Model 1255 frequency response analyzer. Computer modeling of the ac spectra was done using the EQUIVCRT program supplied by PAR with the M383 software. The Material Science and Technology division at LLNL has excellent facilities for electrochemical measurements. The investigators have established a collaborative research program with

CAMD technical staff and have made initial EXAFS measurements using the double beam monochromator beam line port 5A and 5B at CAMD. We are also investigating the solid electrolytes Li/FeS_2 and Li/MnO_2 systems for secondary rechargeable batteries for electric vehicle applications. Several Southern University Physics and Engineering students are associated with this project and are benefiting from these newly developed collaborations with LLNL and CAMD.

Progress

We have measured the ionic conductivities of cerium doped with oxides of the entire rare earth series using ac impedance in air at temperatures of 400°C to 900°C. The maximum conductivity observed (at 600°C) was 1.2×10^{-2} S cm^{-1} for $Ce_{0.8}Sm_{0.2}O_{1.9}$. The conductivity of yttria doped ceria varied substantially with the dopant concentration. Maximum conductivity was observed for the composition $Ce_{1.84}YO_{1.6}O_{1.92}$. In the fall of 1995, we worked with the EXAFS system to study its feasibility for the solid electrolytes. In X-ray absorption spectroscopy, the absorption coefficient is measured as a function of the incident photon energy across the absorption edge of a core level (K or L) electron. The typical spectrum for condensed matter is shown schematically in Figure 1. The region of interest here is the EXAFS region, beginning about 50eV beyond the edge and extending typically a further 1000eV, where the absorption coefficient exhibits sinusoidal oscillations in amplitude. These oscillations arise from the interference between the outgoing part of the photoelectron wave and the part that is backscattered from the neighboring atoms. The EXAFS probes the local structure and does not rely on the presence of long-range order in the sample, making it applicable to crystalline, amorphous, and liquid systems. We made our initial measurements on particular solid electrolytes such as Li/MnO_2 and Li/CoO_2 systems with varied lithium concentrations.

XAS data for the dopant cation in 5 mol%- Sc_2O_3 or 5 mol% Gd_2O_3 doped ceria were measured as fluorescence excitation spectra using a large solid angle ion chamber as the fluorescence detector. All other measurements were made in transmission mode, using ion chambers filled with N_2. All spectra were measured at room temperature.

As mentioned earlier, our goal is to measure the XAS of all the rare earth dopants in ceria using the EXAFS system. In a structural study of fluorite-type oxides (ZrO_2, HfO_2, CeO_2, ThO_2, UO_2, and PuO_2), ceria with different trivalent cations provides a simple model
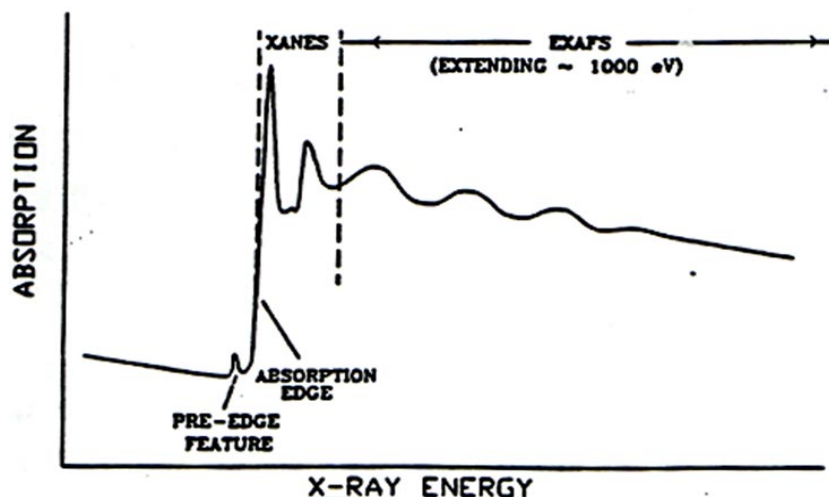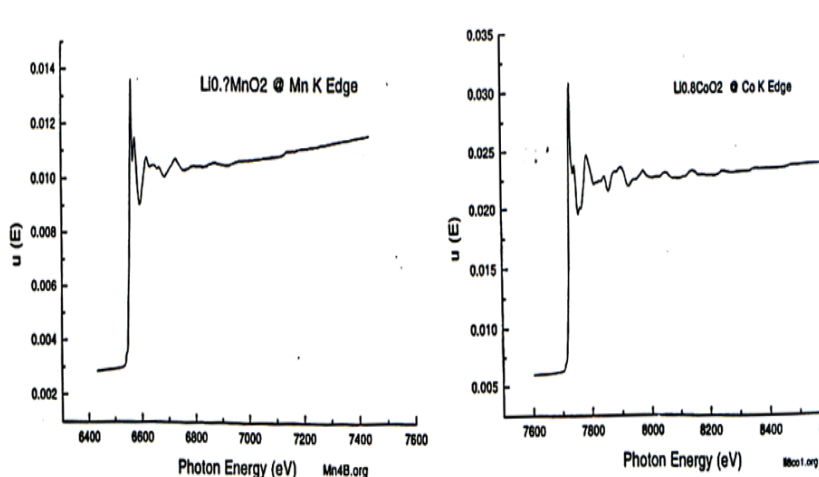

Figure 1. Schematic of a typical transmission EXAFS in a solid.

Figures 2 and 3. Preliminary EXAFS data recorded using EXAFS system at CAMD.

system. In addition, doped ceria is an excellent oxygen ion conductor because of its defect structure at elevated temperatures. A unit cell of CeO_2 consists of eight small cubes containing anions at their corners, with every alternate cube having a cation at its center. When trivalent dopant cations substitutes for Ce^{4+}, one oxygen ion vacancy is introduced for every two cations in order to compensate for the lower cation charge. For a dilute solid solution, an elementary picture of defect structure postulates an equal number MCe-O pairs and isolated MCe, both randomly distributed spatially. We are developing this model to interpret qualitatively the observed electrical properties with dopant concentrations. We wish to point out that, for understanding physical properties such as diffusion and ionic conduction, it is the local structure and short-range order that are important. This information is obtained by measuring X-ray absorption of a probe cation (either host or dopant) at energies near the absorption edge of the probe ion. We will develop several distinct defect/dopant configurations, probably typical of different solid solutions ranges.

References

1. B. Balazas and R. S. Glass, "AC Impedance Studies Of Rare Earth Oxide Doped Ceria," *Solid State Ionics* **76** , pp. 155–162, 1995.

2. Steele, in "High Conductivity Solid Ionic Conductors," ed. T. Takahasi, World Scientific, Singapore, 1989.

3. M. Yashima, N. Ishizawa, and M. Yoshimura, "Science and Technology of Zirconia," Badwal *et al.*, Ed., Lancaster Technomic Publishing, pp. 125–135, 1993.

4. A. V. Chadwick, "EXAFS studies of dopant sites in metal oxides," *Solid State Ionics* **63–65**, pp. 721–727, 1993.

5. G. Anderson and A. S. Nowick, "Ionic Conductivity of CeO_2 with Trivalent Dopants of Different Ionic Radie," *Solid State Ionics* **5**, pp. 547–50, 1981.

First-Principles Computational Studies of Energetic Materials

Principal Investigators: Steven L. Richardson (Howard University) and Christian Mailhiot (LLNL)
**LLNL Collaborator**: Hector Lorenzana

Abstract

The goal of this work is to perform ab initio calculations both at Howard University and LLNL to study the properties of novel energetic materials. Such materials include solid cubane, C_8H_8, and other cubane analogues in which the hydrogen atoms are replaced by other ligands, such as nitro groups. These calculations have utilized state-of-the-art methods that encompass ab initio total energy and ab initio molecular dynamics techniques. Calculations are crucially important to predicting likely synthesis routes as well as to interpreting the experimental properties. A synergistic theoretical and experimental effort also exists between Howard University and LLNL that aims to study some of these energetic materials properties under pressure.

Objectives

The discovery of new materials has been a critical factor in driving advances in material technologies. These "novel" materials have been recognized by their superiority in their mechanical, energetic, and electronic properties. The emphasis of the proposed work is on exploring novel energetic materials designed from first-row light elements: C, N, and O. Specifically, we have recently investigated cage-like carbon-based structure, solid cubane C_8H_8 (Figure 1). This material stores energy through its highly strained bonds that deviate from the normal C-C bond angle of 109.8° in the tetrahedral SP^3 form of carbon. The bond angle in cubane is nearly 90°, causing the molecule to be highly energetic. Nitro-substitutions (NO_2) for the H atoms are other energetic variants of cubane.

Little work exists on the structural and electronic properties of the cubane solid or the nature of its crystalline form. Thus, the thrust of this effort is to apply *ab initio* total energy and molecular dynamic methods to calculate structural, electronic, and vibrational properties of solid cubane. We also plan to calculate high pressure properties, including structural phase transitions.

• solid cubane (C_8H_8)
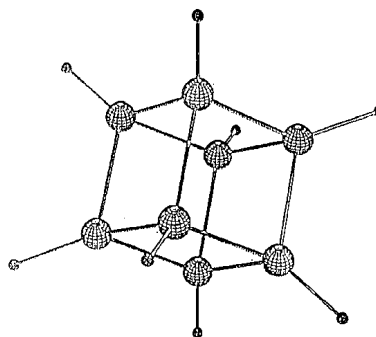
Bonding Schemes:

    C: sp (polyyne or carbyne)
    C: sp^2 (polyacetylene, graphite, fullerenes)
    C: sp^3 (diamond, cubane)

Figure 1. Simpler caged carbon-based units.

Progress

We used the plane wave local density approximation with *ab initio* pseudopotentials developed by Troulier and Martins[1] to calculate the structural and electronic properties of crystalline cubane (C_8H_8).[2] In particular, we have computed the lattice constant, bulk modulus, and cohesive energy for cubane and compared these data with the experimental data that are available.[3] The electronic band structure and total valence charge densities were also studied.

Additionally, we are closely tied to an experimental effort studying the characteristics of novel energetic materials as well as synthesis methods. The recently developed laser-heated diamond-anvil-cell (DAC) offers powerful diagnostic capabilities as well as a promising synthesis route of some of these novel high-pressure phases (Figure 2). Preliminary measurements in nitrogen demonstrate the technique's capability to characterize internal vibrational modes, electronic changes, and phase transitions. Current plans are to apply these techniques to cubane-derived materials.
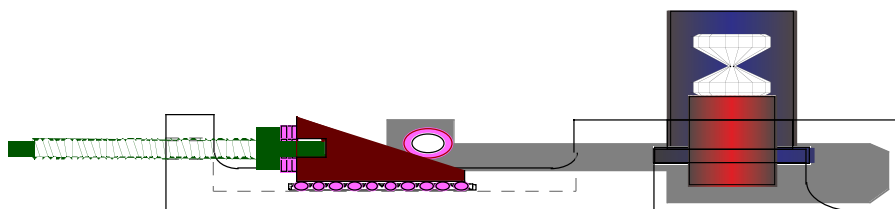

Figure 2. Diamond Anvil Cell. Generates millions of atmospheres of pressure.

References

1. N. Troullier and J. L. Martins, *Phys. Rev. B* **46**, p. 1754, 1992.

2. P. E. Eaton and T. W. Cole, Jr., *J. Am. Chem. Soc*, **86**, p. 3158, 1964.

3. E. M. Fleischer, *J. Am. Chem. Soc.* **86**, p. 3889, 1964.

Charge Exchange Measurements Relevant for Plasma Physics

Principal Investigators: Joseph Johnson (Florida A&M University) and Dieter Schneider (LLNL)
Students: J. McDonald, J. Steiger, and B. Beck

Abstract

Studies of slow collisions between highly charged or bare high-Z ions and gaseous (atomic, molecular) or solid targets are important for understanding fusion plasmas and ion-surface-interaction phenomenon relevant to wall effects in heavy ion fusion driver concepts. Highly charged low energy ions are produced in transport beam lines following wall sputtering, and their effect on the beam transport can be significant. Understanding these collisions requires knowledge of charge exchange cross sections, recombination dynamics, and decay processes. In fusion plasmas, charge exchange and radiative de-excitation channels are important for accounting for trace elements and for diagnosing plasma processes. In FY94, we started to perform charge exchange measurements with slow highly charged ions in low density gas targets using a Penning ion trap, and the first results for decay rates for ions ranging from Be^+ to Th^{76+} were obtained.

Objectives

The combination of heavy ions with very high charge plus very low energies is rare in nature, but will be encountered in planned fusion energy devices, such as the "International Thermonuclear Experimental Reactor" (ITER) in ion sources and in astrophysical events. New experimental studies of very highly charged ions in ion traps make the careful investigation of charge exchange rates essential, since these rates determine the storage time of the ions in the trap at a given residual neutral density. Furthermore, these measurements provide a test of the theories of electron transfer in ion-neutral collisions. In low-energy atomic collisions of highly charged ions, electrons are captured into high n states, which generally decay by cascade transitions. It is noted that unusual state populations can be created via capture and radiative decay. Many such "inverted"

populations are also interesting for x-ray laser schemes. The goal of the experimental effort is to provide benchmark data for charge exchange cross sections for slow highly charged ions.

Progress

Electron capture from H_2 to Xe^{q+} and Th^{q+} ions ($35 \leq q \leq 80$) has been studied at mean ion energies estimated to be $< 5q$ eV, where q is the ion charge state. These measurements were carried out in a Penning ion trap coupled to the Lawrence Livermore National Laboratory Electron Beam Ion Trap (LLNL EBIT) . This arrangement allows for the study of highly-charged ions at low energies under well-controlled conditions.[1] The charge exchange rates were measured in the trap via the decrease in the initial ion stochastic voltage signal and the gain in signal of ions in adjacent charge state. The measured rates, which agree well with previously published results for Be^{2+} and Ar^{11+} ions, are compared to theoretical predictions. The results thus far indicate that theoretical treatments and parameterizations applied to lower charge states extrapolate well to higher charge, particularly for the q-dependence of the electron transfer cross section.

References

1. D. Schneider, D. A. Church, G. Weinberg, J. Steiger, B. B. Beck, J. McDonald, E. Magee, and D. Knapp, *Rev. Sci. Instrum.* **65**, p. 3472, 1994.

CP Violation at the SLAC/LBL/LLNL B-Factory

Principal Investigators: Dennis Judd, Kwang Paick, David Wagoner, and Mei Gui (Prairie View A&M University) and Karl van Bibber (LLNL)

LLNL Collaborators: Xiaorong Shi, Torre Wenaus, and Douglas Wright

Student: George Aduo

Abstract

The SLAC/LBL/LLNL B-Factory is an approved High Energy Physics colliding beam facility committed to the observation of CP violation in the neutral B meson system. CP violation is a necessary ingredient in cosmological mechanisms for producing an excess of matter over antimatter in the early universe. Besides the possible cosmological significance, the mechanism for producing CP violation, in the Standard Model of elementary particle physics, is not completely understood. Studies at the B-Factory could provide the first observation of CP violation in B mesons and will probe the CP violation mechanism. We are in the process of designing and analyzing the performance of the muon/neutral hadron detector subsystem for BaBar, the B-Factory detector. This detector subsystem is important for distinguishing the particle/anti-particle content of B mesons and for reconstructing B decays into CP eigenstates.

Objectives

Since the initial discovery of CP violation in neutral kaons in 1964,[1] the Standard Model mechanism invented to describe it has remained untested. The B-Factory is designed to make an unambiguous and over-constrained test of this mechanism by reconstructing *B* meson decays from electron-positron annihilation. If the results contradict the Standard Model, the multiple independent measurements could indicate the source of the deviation. This may be the first look at new physics beyond the Standard Model. The B-Factory accelerator is now under construction, with a scheduled start-up at the end of 1998.

In order to observe CP violating asymmetries, one of the two primary *B* mesons must be fully reconstructed, the other must be tagged by its weak decay products, and the primary vertex of both must be measured. BaBar,[2] the B-Factory detector depicted in

Figure 1, is therefore a general purpose, high precision detector consisting of a silicon strip micro-vertex detector, central tracking drift chamber, Cerenkov light-based particle identification system, electromagnetic crystal calorimeter, magnet coil, and instrumented iron flux return (IFR). The BaBar collaboration recently received approval of their Technical Design Report[3] for the detector, and is preparing a detailed design of each subdetector component.

The IFR subdetector serves two purposes. The magnetic flux generated by the large superconducting central coil is returned through a hexagonal barrel and endcap configuration of steel plates. The steel plates also act as a hadron absorber as well as a path for the magnet field. By placing charged particle detectors, resistive plate chambers (RPC), between the layers of steel, the flux return provides muon and hadronic shower detection capabilities. Our primary objective is the detailed design of the IFR system and analyzing its physics capabilities.
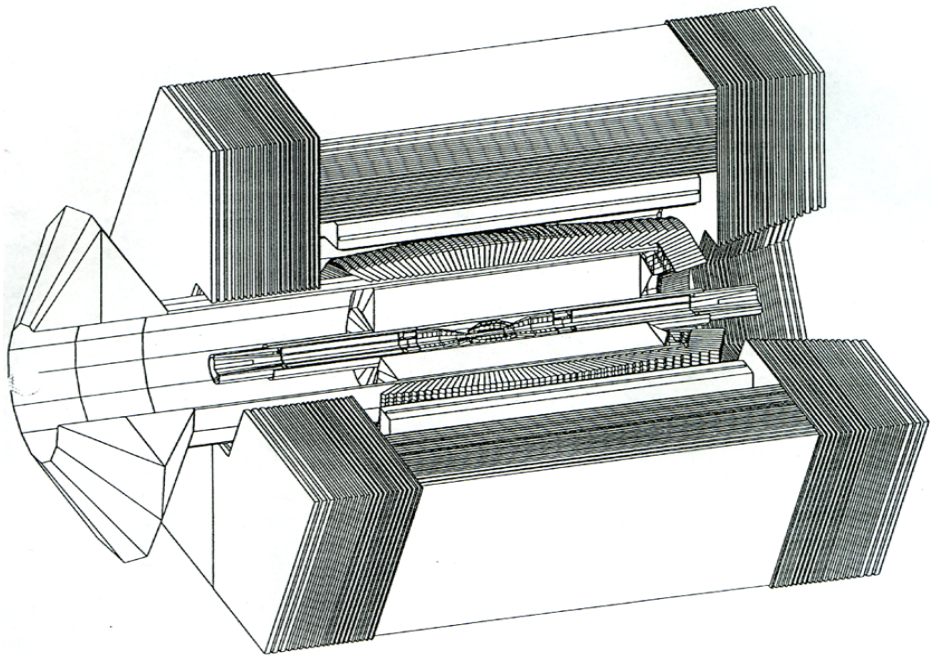
_____

Figure 1. BaBar detector at the SLAC/LBL/LLNL B-Factory.

Progress

The physics performance of the BaBar detector subsystems is determined from detailed Monte Carlo simulations of the primary particles and their interaction with the detector. A large portion of the software dedicated to simulating the BaBar detector was developed by LLNL physicists.[4,5] The performance of the present IFR configuration should be verified and further optimized with a more detailed description of the detector geometry and realistic detector response functions. Implementing these reality enhancements will require modifications to the reconstruction algorithms for muon and hadron identification. In addition, we plan to extend the level of sophistication of these algorithms and implement a multivariate tagging analysis based on reconstructed muon parameters.

Our initial activities focused on integrating Prairie View A&M University collaborators into the sophisticated BaBar simulation framework. We established Prairie View computing resources, both hardware and an extensive software base, on-site at LLNL and at Prairie View A&M University. After becoming familiar with the simulation software, Prairie View developed a significantly more accurate and detailed model of the RPC chambers. We also have begun to use a new system for distributing and sharing the software, which will improve our ability to work cooperatively from remote sites.

In FY96, we will build on the experience gained in the previous year. Prairie View will take responsibility for one of the existing reconstruction algorithms, both extending and enhancing it. We will explore the use of object-oriented programming in C++ for implementing the sophisticated reconstruction algorithms. We will also contribute new physics analyses based on IFR detector output.

References

1. K. Kleinknecht, "CP violation and K0 decays," *Ann. Rev. Nucl. Science* **26**, p. 1, 1976.

2. BaBar Collaboration, *BaBar Technical Design Report*, SLAC-R-95-457, March 1995.

3. BaBar Collaboration, Letter of Intent for the Study of CP Violation and Heavy Flavor Physics at PEP-II, SLAC-443, June 1994.

4. Douglas Wright, "BEGET: The B-Factory Event Generator," BaBar Note #149, 1994.

5. T. Wenaus, "The bbsim Geant Simulation for BaBar," http://www.slac.stanford.edu/BF/doc/Computing/Simulation/bbsim.html.

Section III. Publications and Abstracts Produced by the 1994–95 Research Collaborations Program

A. Asfaw, C. Back, T. Barbee, L. Da Silva, S. Glenzer, **L. Klein**, **R. Lee**, J. Moreno, A. Wan, N. Woolsey, C. Mosse, B. Talin, R. Stamm, A. Calisti, and J. Koch, "Photopumping and Redistribution in Laser Produced Plasma," APS 37th Annual Meeting of the Division of Plasma Physics **40**, No. 11, p. 1724.

A. Asfaw, **R. Shepherd**, **R. Lee**, J. Koch, and N. Woolsey, "Time Resolved Soft X-ray Measurement from Femtosecond Laser Plasma," APS 37th Annual Meeting of the Division of Plasma Physics **40**, No. 11, p. 1722.

P. Beiersdorfer, S. R. Elliott, A. Osterheld, Th. Stöhlker, **J. Autrey**, G. Brown, **A. J. Smith**, and K. Widmann (submitted), "Search for 1s2s $^3S_1 - {}^3P_2$ Decay in U^{90+}," *Phys. Rev. A.*

P. Beiersdorfer, K. Widmann, V. Decaux, A. Osterheld, M. Bitter, K. Hill, S. von Goeler, and **A. Smith** (in press), "Detailed Measurements and Modeling of the $n=3$ to $n=1$ Spectrum of He-like Argon (Ar^{16+})," *Bull. Am. Phys. Soc.*

M. Bennahmias, **H. B. Radousky**, **M. Buford**, **A. Kebede**, M. McIntyre, T. J. Goodwin, and R. N. Shelton, "Magnetic Studies of Ta Doping in $PrCe_{0.5}Sr_2Cu_2NbO_{10}$," *Phys. Rev. B.*, in press.

K.-T. Chen, **T. D. Journigan**, **S. Lecointe**, J. Tong, **A. Burger**, **L. D. DeLoach**, R. H. Page, and **S. A. Payne**, "Diffusion of chromium and its solubility in ZnSe crystals for Cr^{+2}:ZnSe tunable laser application," the Sixth Eastern Region Conference on Crystal Growth, ACCG/east-95, October 15–18, 1995, Atlantic City, NJ.

K.-T. Chen, Y. Zhang, S. U. Egarievwe, M. A. George, **A. Burger**, C.-H. Su, Y.-G. Sha, D. C. Gillies, and S. L. Lehoczky, "Post-Growth Annealing of CdS Crystals Grown by Physical Vapor

Transport," presented at the Eleventh International Conference of Crystal Growth, ICCG XI, The Hague, Holland, 1995. (Accepted for publication in the *Journal of Crystal Growth* as a special issue of the Proceedings of ICCG XI.)

S. Chittipeddi, V. C. Kannan, and **B. Rambabu**, "Integrity of Shallow Junction CMOS Structures with Ti/TiN/Al-Si-Cu and Ti/TiN/Al-Cu Contact Metallization," *Solid State Electronics* **38**, pp. 23–28, 1995.

T. George, **R. Bobba**, and S. Cehl, "Preparation and Character-ization of Solid Electrolytes for Solid Oxide Fuel Cells," NASA Annual Meeting, Marshal Space Research Center, MS, 1995.

S. Glenzer, Th. Wrubel, S. Buscher, H.-J. Kunze, L. Godbert, A. Calisiti, R. Stamm, B. Talin, J. Nash, **R. Lee**, and **L. Klein**, "Spectral Line Profiles of n=4 to n=5 transitions in C_{IV}, N_V and O_{VI}," *J. Phys. B: At. Mol. Opt. Phys.* **27**, p. 5507, 1994.

L. Godbert, A. Calisti, R. Stamm, B. Talin, J. Nash, **R. Lee**, **L. Klein**, S. Glenzer, and H.-J. Kunze, "Plasma Spectroscopy of n=4 to 3 C_{IV} and N_V Lines in Hot and Dense Plasmas," *Phys. Rev E* **49**, p. 5889, 1994.

L. Godbert, A. Calisti, R. Stamm, B. Talin, **R. Lee**, and **L. Klein**, "Plasma Diagnostics with Spectral Line Shapes," *Phys. Rev. E* **49**, p. 5644, 1994.

D. J. Hylton and **N. J. Snyderman**, "Analytic Basis set for high-Z atomic QED calculations: He-like ions," submitted to *Phys. Rev A*.

J. J. Jia, T. A. Callcott, **A. Asfaw**, J. A. Carlisle, L. J. Terminello, D. L. Ederer, and R. C. C. Perera, "Occupied Electronic States of Casi2 and Casi: Soft X-ray Fluorescence Spectroscopy," *Phys. Rev. E* **15**, 1995.

J. J. Jia, T. A. Callcott, **A. Asfaw**, J. A. Carlisle, L. J. Terminello, D. L. Ederer, F. J. Himpsel, and R. C. C. Perera, "X-ray Raman Scattering in h-BN Observed by Soft X-Ray Fluorescence Spectroscopy," submitted to *Phys. Rev. Lett*.

J. J. Jia, T. A. Callcott, **A. Asfaw**, D. L. Ederer, R. C. C. Perera, J. A. Carlisle, L. J. Terminello, and F. J. Himpsel, "Resonant Inelastic Raman Scattering Observed near B K edge in h-BN and B_2O_3 by Soft X-ray Fluorescence Spectroscopy," *APS* **40**, No. 1, p. 337, March 1995

J. Jimenez-Mier, D. L. Ederer, U. Diebold, T. A. Callcott, L. Zhou, J. J. Jia, J. Carlisle, E. Hudson, L. J. Terminello, **A. Asfaw**, F. J. Himpsel, and R. C. C. Perera, "Stoichiometric-Dependent Inelastic and Resonant Scattering in Titanium and its Oxides," *APS* **40**, No. 1, p. 389, March 1995.

J. Koch, K. Estabrook, J. Bauer, C. Back, **L. Klein**, A. Rubenchick, E. Hsieh, R. Cook, B. MacGowan, J. Moreno, D. Kalantar, and **R. Lee**, "Time-Resolved X-ray Imaging of High-Power Laser-Irradiated Under-Dense Silica Aerogels and Agar Foams," *Physics of Plasmas* (to be published, October 1995).

J. A. Koch, C. A. Back, C. A. Iglesias, D. L. McWilliams, R. C. Cauble, E. J. Hsieh, N. Kornblum, N. C. Woolsey, J. C. Moreno, **A. Asfaw**, J. K. Nash, F. J. Rogers, and **R. W. Lee**, "Time-Resolved Temperature Measurements of Radiatively Heated Tamped MgO Foils by Ka Absorption Spectroscopy," *JQRST* **54**, No. 1/2, pp. 227–236, 1995.

K. Langry and **R. Bobba**, "Ionic Optrodes: Role in Fiber Optic Sensor Technologies," *Solid State Ionics*, accepted for publi-cation, 1996.

C. LeJune, Jr., **R. Bobba**, B. Balazs, and **R. S. Glass**, "Effect of Ionic Radius on the Structural Integrity of Doped Ceria, "10th International Conference on Solid State Ionics, Singapore, December 1995.

M. J. McIntyre, **M. J. Bennahmias**, T. J. Goodwin, C. C. Hoellwarth, A. F. Bello, **C. M. Buford**, **A. Kebede**, R. N. Shelton, and **H. B. Radousky**, "Magnetism in $(Pr_{1.5}Ce_{0.5})Sr_2Cu_2Nb_{1-x}Ta_xO_{10}$," *Bull. of the APS* **40**, 1995.

C. Mosse, A. Calisti, M. Koubiti, R. Stamm, B. Talin, J. Koch, **R. Lee**, and **L. Klein**, "Redistribution of Resonance Radiation in Hot, Dense Plasmas," (to be submitted to *Phys. Rev. E*).

C. Mosse, A. Calisti, R. Stamm, B. Talin, J. Koch, **A. Asfaw**, N. Woolsey, C. Back, **R. Lee**, J. Seeley, and **L. Klein**, "X-ray Laser Photopumped Resonance Fluorescence," (submitted to *Phys. Rev. E*).

R. Shepherd, **A. Asfaw**, J. Koch, **R. Lee**, D. Price, B. Young, A. Osterheld, M. Foord, R. More, and R. Stewart, "Sub-kilovolt, broadened x-ray emission from short pulse laser-produced plasma at the Lawrence Livermore National Laboratory Ultra Short Pulse Laser," APS 37th Annual Meeting of the Division of Plasma Physics **40**, No. 11, p. 1661.

R. Shepherd, **A. Asfaw**, D. Price, M. Foord, R. Walling, and **R. Lee**, "The Measurement of Sub-picosecond Laser Pulse X-Ray Conversion Mechanisms," (to be submitted to *Phys. Rev. Lett.*)

A. J. Smith, **P. Beiersdorfer**, V. Decaux, K. Widmann, A. Osterheld, and **M. Chen**, "Measurement of Doubly Excited Levels in Lithiumlike and Berylliumlike Cobalt," *Phys. Rev. A* **51**, p. 2808, 1995.

A. J. Smith, **P. Beiersdorfer**, V. Decaux, K. Widmann, A. Osterheld, and **M. Chen**, "Measurement of Dielectronic Recombination Resonances in Heliumlike and Lithiumlike Cobalt," Proceedings of the 19th International Conference on the Physics of Electron Atom Collisions, Whistler, BC, Canada, July 26–August 1, 1995.

A. J. Smith P. Beiersdorfer, V. Decaux, K. Widmann, **K. J. Reed**, and **M. Chen**, "Measurement of the Contributions of High-n Satellites to the Kb Lines of He-like Ar^{16+}," (submitted to *Phys. Rev. A*).

B. Talin, A. Calisti, L. Godbert, R. Stamm, **R. W. Lee**, and **L. Klein**, "Frequency Fluctuation Model for Line Shape Calculations in Plasma Spectroscopy," *Phys. Rev. A* **51**, p. 1918, 1995.

N. Woolsey, **A. Asfaw**, B. Hammel, C. Keane, C. Back, **R. Lee**, A. Calisti, C. Mosse, R. Stamm, B. Talin, J. Wark, and **L. Klein**, "Spectroscopic Study of Compressed High Energy Density Matter," (submitted to *Phys. Rev. E*).

N. C. Woolsey, **A. Asfaw**, C. A. Back, R. Cauble, S. Glenzer,
E. Hsieh, J. S. Wark, and **R. W. Lee**, "Strain Measurements
of Shock Compressed Solids at the Lattice Scale," APS 37th Annual
Meeting of the Division of Plasma Physics **40**,
No. 11, p. 1854.

N. C. Woolsey, **A. Asfaw**, **R. W. Lee**, J. S. Wark, and
R. Cauble, "Measurement of Near M-bar Shock Fronts in Crystals by
X-ray Diffraction," APS Topical Conference on Shock Compression
of Condensed Matter **40**, No. 6, July 1995.

N. C. Woolsey, **R. W. Lee**, **A. Asfaw**, C. A. Back, S. Glenzer,
B. Hammel, D. Kalantar, J. Koch, J. Moreno, **L. Klein**, B. Talin,
R. Stamm, L. Godbert, and C. Mosse, "Spectroscopy of argon doped
indirectly driven ICF capsules," APS 37th Annual Meeting of the
Division of Plasma Physics **40**, No. 11, p. 1670.

L. Zhou, T. A. Callcott, J. Jia, D. L. Ederer, **A. Asfaw**, and
R. C. C. Perera, "The Sulfur $L_{2,3}$ Emission Spectra of TM-S
Compounds," *APS* **40**, No. 1, p. 841, March 1995.

Section IV. Projects and Participants in the 1994–95 Research Collaborations Program

Project	HBCU	Faculty/Students	LLNL P.I. (Collaborator)	LLNL Division
Development of Cr^{2+}-doped II-VI Hosts as Mid-Infrared Lasers	Fisk University	1 faculty 3 grad students 2 undergrad students 1 post-doc	S. Payne *R. Page* *K. Schaffers* *L. DeLoach*	Lasers
X-ray Spectroscopy on the Electron Beam Ion Traps	Morehouse College	1 faculty 3 students	P. Beiersdorfer *V. Decaux* *K. Widmann* *J. López-Urrutia*	N Division
Magnetic Impurity Studies of High T_c Superconductors	North Carolina A&T University	1 faculty 2 students	H. Radousky *M. Bennahmias*	H Division
Unified Formulas for Electron-Impact Excitation Cross Sections and Rate Coefficients	Southern University	1 faculty 3 students	M. Chen K. Reed	V Division V Division
Turbulence Measurements in Fuel Injection Emulation	Florida A&M University	1 faculty	C. Westbrook R. Carling	H Division SNL
Analytic Basis Set for High-Z Atomic QED Calculations: Heavy Helium-Like Ions	Spelman College	1 faculty 2 students	N. Snyderman	N Division
Investigation of Organic Nonlinear Optical Crystals for Harmonic Frequency Conversion and Electro-Optics	Alabama A&M University	1 faculty 1 grad. student	H. Lee *J. Cooke*	H Division
Studies in High Energy Density Plasmas and X-ray Fluoresence of Condensed Matter	Howard University	1 faculty 1 post-doc	R. Lee *R. Shepherd*	D&NT V Division
Studies in High Energy Density Plasmas	Howard University	1 faculty 2 students	R. Lee *R. Shepherd* *R. Ward*	D&NT V Division
Development of Solid Electrolyte Materials for Gas Phase Sensors and Fuel Cells	Southern University	1 faculty 3 students	R. Glass *G. Balazs*	C&MS
First-Principles Computational Studies of Energetic Materials	Howard University	1 faculty	C. Mailhiot *H. Lorenzana*	H Division

Project	HBCU	Faculty/Students	LLNL P.I. (Collaborator)	LLNL Division
Charge Exchange Measurements Relevant for Plasma Physics	Florida A&M University	1 faculty 3 students	D. Schneider	N Division
CP Violation at the SLAC/LBL/LLNL B-Factory	Prairie View A&M University	3 faculty 2 students 1 post-doc	K. van Bibber *X. Shi* *T. Wenaus* *D. Wright*	N Division